

Article

Chemo- and regioselective benzylic C(sp³)-H oxidation bridging the gap between hetero- and homogeneous copper catalysis

Shantanu Nandi,
Shuvam Mondal,
Ranjan Jana

rjana@iicb.res.in

Highlights

Catalytic strategy for
chemo- and
regioselective benzylic C–
H activation

Bulk copper catalysis
merging with
photocatalysis

Reusable copper catalyst

Reaction demonstrated in
commercial copper bottle
without external catalyst

Nandi et al., iScience 25,
104341
May 20, 2022 © 2022 The
Authors.
[https://doi.org/10.1016/
j.isci.2022.104341](https://doi.org/10.1016/j.isci.2022.104341)

Article

Chemo- and regioselective benzylic C(sp³)-H oxidation bridging the gap between hetero- and homogeneous copper catalysisShantanu Nandi,¹ Shuvam Mondal,¹ and Ranjan Jana^{1,2,*}

SUMMARY

Selective C–H functionalization in a pool of proximal C–H bonds, predictably altering their innate reactivity is a daunting challenge. We disclose here, an expedient synthesis of privileged seven-membered lactones, dibenzo[*c,e*]oxepin-5(7H)-one through a highly chemoselective benzylic C(sp³)-H activation. Remarkably, the formation of widely explored six-membered lactone via C(sp²)-H activation is suppressed under the present conditions. The reaction proceeds smoothly on use of inexpensive metallic copper catalyst and di-*tert*-butyl peroxide (DTBP). Owing to the hazards of stoichiometric DTBP, further, we have developed a sustainable metallic copper/rose bengal dual catalytic system coupled with molecular oxygen replacing DTBP. A 1,5-aryl migration through Smiles rearrangement was realized from the corresponding diaryl ether substrates instead of expected eight-membered lactones. The present methodology is scalable, applied to the total synthesis of cytotoxic and neuroprotective natural product alterlactone. The catalyst is recyclable and the reaction can be performed in a copper bottle without any added catalyst.

INTRODUCTION

Despite an impressive array of C–H functionalization reported in the last decades, maintaining a high degree of chemo-, regio-, and stereoselectivity in a plethora of ubiquitous C–H bonds remains a major challenge (Dalton et al., 2021; Gandeepan et al., 2019; Yi et al., 2017). The chemo- and regioselective transformation in a pool of vulnerable C–H bonds in nondirected fashion through the judicious choice of the catalytic system is a prime research area (Khake and Chatani, 2020; Lerchen et al., 2018). In the past, copper (Rout et al., 2012), iron (Lu et al., 2017), palladium-catalyzed (Ju et al., 2013), or metal-free (Feng et al., 2012) intermolecular acetoxylation of benzylic C–H bonds have been reported where the reaction proceeds through the formation of a putative metal-carboxylate or acyloxy radical species. The Stahl group and others reported copper-catalyzed intermolecular benzylic C–H functionalization for the synthesis of pharmacophores from feedstock chemicals (Chi et al., 2019; Hu et al., 2020a; Liu et al., 2020; Vasilopoulos et al., 2017; Wang et al., 2019). The Ritter group reported a copper (II)-catalyzed synthesis of benzylic alcohols from alkyl arenes employing bis(methanesulfonyl)peroxide as an oxidant followed by hydrolysis (Tanwar et al., 2019). Synthesis of benzyl esters was unveiled by the Patel group using Cu(II)/TBHP and excess amount of methylarenes (Rout et al., 2012, 2014). However, the scope of benzylic activation with equimolar amount of alkylarene as coupling partner is still limited. Alternatively, intramolecular C–H bond oxidation by a tethered carboxylic acid is emerging to provide lactones directly (Cianfanelli et al., 2020; Das et al., 2020; Zhuang and Yu, 2020). A copper-catalyzed five- and six-membered lactone formation through intramolecular benzylic C–H acetoxylation was reported by the Bois group (Sathyamoorthi and Du Bois, 2016). Alternatively, the Martin group accomplished the synthesis of a six-membered lactone from *ortho*-aryl benzoic acid through copper-catalyzed C(sp²)-H bond activation (Gallardo-Donaire and Martin, 2013). Subsequently, this protocol was extrapolated by several groups using other metals or metal-free conditions via the single electron activation of aryl carboxylic acids (Scheme 1A). (Bhunja et al., 2019; Dai et al., 2015; Li et al., 2013, 2018; Ramirez et al., 2015; Shao et al., 2018; Tao et al., 2018; Wang et al., 2014; Yang et al., 2018; Zhang et al., 2018a, 2018b) Although soluble copper complexes or copper nanoparticles (CuNPs) have been used for the C–H functionalization (Aneeja et al., 2020; Guo et al., 2015b), the use of inexpensive bulk Cu catalyst is extremely rare (Guo et al., 2015a; Meng et al., 2020). Recent efforts to bridge the gap between hetero- and homogeneous catalysis for improved catalytic activity, selectivity, and cost efficiency

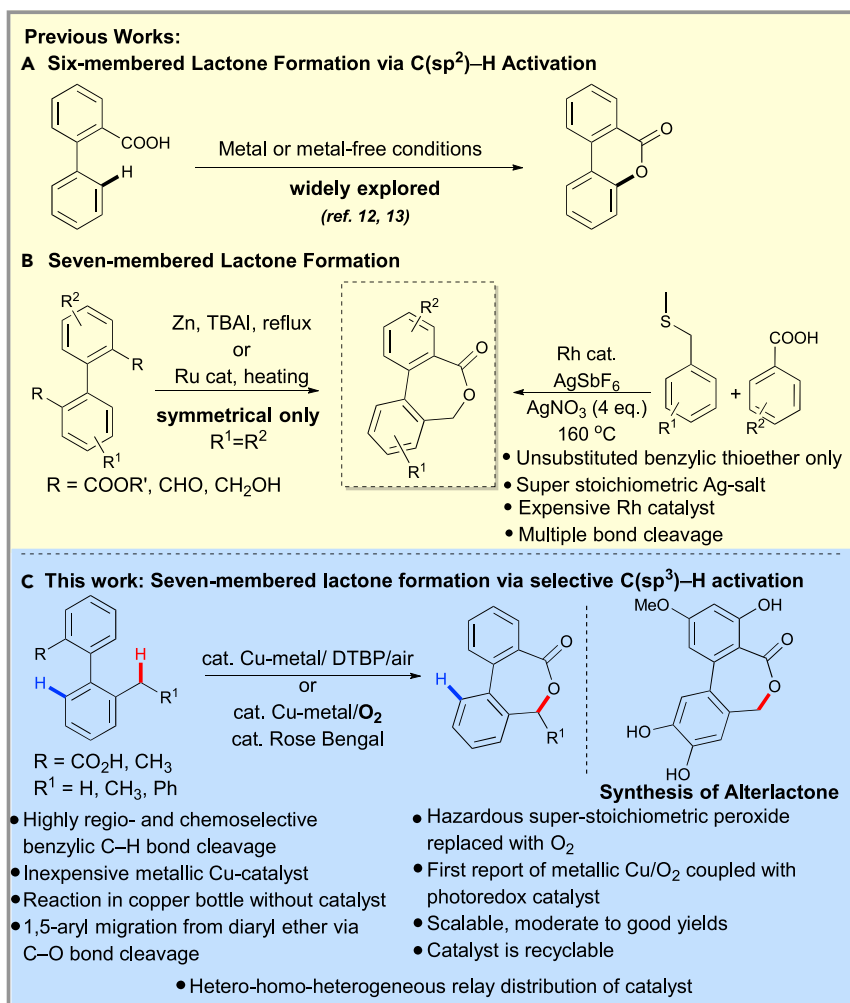
¹Organic and Medicinal Chemistry Division, CSIR-Indian Institute of Chemical Biology, Raja S. C. Mullick Road, Jadavpur, Kolkata 700032, West Bengal, India

²Lead contact

*Correspondence: rjana@iicb.res.in

<https://doi.org/10.1016/j.isci.2022.104341>





Scheme 1. Approaches to access biaryl lactones

is prevailing (Copéret et al., 2003; Cui et al., 2018; Liu and Corma, 2018; Van Velthoven et al., 2020). Particularly, inexpensive bulk copper catalysis for the chemoselective sp³ vs sp² C-H activation has not been explored. Only a palladium-mediated chemoselective sp³ vs sp² C-H activation was disclosed by the Kozłowski group (Curto and Kozłowski, 2015; Hong et al., 2019).

Dibenzoaxepinones and their analogs are found in natural products and bioactive molecules exhibiting antitumor, tyrosine kinase inhibitor, cytotoxic, and antimicrotubule activity (Figure 1). (Altemöller et al., 2009; Aly et al., 2008; Colombel et al., 2010; Höller et al., 2000; Wu et al., 2008) Typically, this dibenzo [c,e]oxepin-5(7H)-one motif is constructed by a sequence of biaryl coupling and C-O bond-forming lactonization (Scheme 1B). (Dana et al., 2018; Miyagawa and Akiyama, 2018; Omura et al., 2009; Tang et al., 2020b) However, these methods are either limited to the symmetrical biaryls or prefunctionalized benzyl alcohols for lactone formation. Recently, Tang et al. reported the synthesis of 7-membered biaryl lactones via iodolactonization of electron-deficient olefins (Tang et al., 2020a). A rhodium(III)-catalyzed cross-coupling of benzylic thioethers and aryl carboxylic acids exploiting two directing groups was reported by the Shi group (Scheme 1C). (Zhang et al., 2015) However, synthesis of benzylic thioether from the corresponding bromide was necessary where no benzylic substitution was tolerated. Surprisingly, the formation of seven-membered biaryl lactone through simple intramolecular benzylic C-H oxidation by the carboxylic acid is not explored. This could be attributed to the fact that although benzylic sp³ C-H bond cleavage is energetically favorable compared to sp² C-H bond (85–90 kcal/mol vs 110–115 kcal/mol) (Blanksby and El-lison, 2003; Curto and Kozłowski, 2015), the metal-catalyzed seven-membered ring formation is disfavored

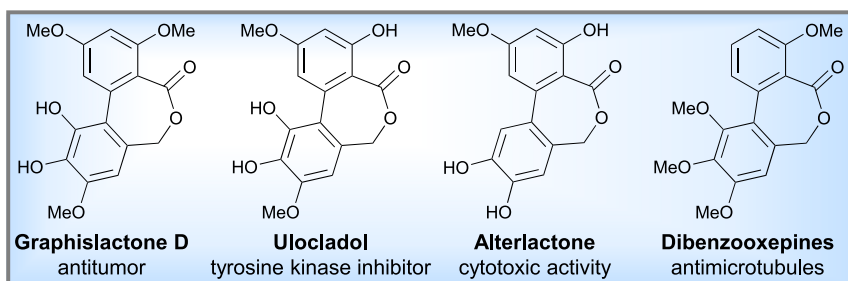


Figure 1. Biologically important dibenzooxepinone core

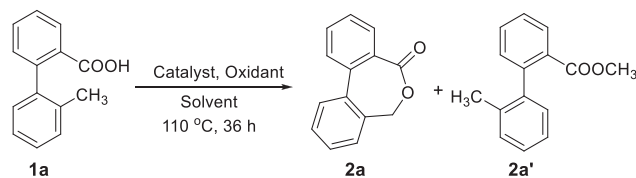
compared to the corresponding six-membered ring due to the involvement of putative eight-membered metallacycle. We hypothesized that contrary to the conventional two-electron pathway, a single electron activation of the aryl carboxylic acid followed by hydrogen atom transfer (HAT) might activate the benzylic C–H bond selectively furnishing seven-membered lactones. If succeeded, a series of dibenzooxepinones could be synthesized via this unusual disconnection approach which is prevalent in natural products and pharmaceuticals. Intrigued by these precedents, we were motivated to explore an orthogonal reaction for the formation of dibenzooxepinone through intramolecular benzylic C–H oxidation of the corresponding 2'-alkyl-[1,1'-biphenyl]-2-carboxylic acid **1**. Furthermore, exploiting the subtle disparity in chemical reactivity of the two alkyl groups, similar dibenzo[c,e]oxepin-5(7H)-ones were obtained from the corresponding 2,2'-dialkyl-substituted biaryls. Remarkably, inexpensive copper powder is used with organic peroxide as an oxidant. Fascinatingly, hazardous peroxide has been replaced with molecular oxygen merging copper powder catalyst with organic photocatalyst, rose bengal. Though there are some reports for copper salt/photoredox (Barzanò et al., 2020; Shi et al., 2020; Tao et al., 2017; Zheng et al., 2020) or copper/O₂ systems (Liang et al., 2019), to the best of our knowledge, this is the first report for bulk metallic copper/photocatalysis to couple with O₂ in benzylic C–H oxidation. Remarkably, a highly reactive, substrate-dependent soluble catalyst is formed from the copper powder during the reaction to achieve high degree of chemoselective sp³ vs sp² C–H oxidation (Scheme 1D). The corresponding diaryl ether undergoes a carboxylic acid radical-assisted 1,5-aryl migration via *ortho* C–O bond cleavage. Finally, the heterogeneous catalyst is precipitated out and recovered for subsequent runs by simple filtration offering dual benefits of homo- and heterogeneous catalyst.

RESULTS AND DISCUSSION

Investigation of reaction conditions

To create a competitive innate C–H activation scenario, we designed 2'-methyl-[1,1'-biphenyl]-2-carboxylic acid **1a** as a model substrate. To our delight, we achieved 52% of our desired product along with the corresponding methyl ester **2a'** using catalytic CuI in combination with di-tert-butyl peroxide (DTBP) (Tran et al., 2014; Xia et al., 2013). Presumably, **2a'** is formed by the radical-radical coupling of methyl radical generated from the DTBP and carboxyl radical. To improve the yield of **2a** and diminish the formation of **2a'** systematically, the metal catalysts, oxidants, and solvents were examined (Table 1). α,α,α -trifluorotoluene was found to be the best solvent. Surprisingly, we found copper(II) catalysts as well as other oxidants such as TBHP, DCP to be inferior to copper(I)/DTBP. Next, we focus to use inexpensive copper(0) metal as a catalyst which eventually oxidized to higher oxidation states *in situ*. Gratifyingly, metallic copper (mesh size 425 μ m) with DTBP furnished **2a** in 82% yield on heating at 110°C for 36 h along with the formation of deleterious product **2a'** (Entry 11, Table 1). We speculated that the addition of an external radical trapping agent might capture the methyl radical to sieve the formation of **2a'**. As hypothesized, the addition of 2.0 equiv of TEMPO suppressed the formation of **2a'** with an improved 83% yield of the desired lactone product **2a** (Entry 12, Table 1). Notably, reaction with commercial CuNPs (25nm particle size) also furnished the reaction in similar yields (Entry 10, Table 1) whereas reaction under argon or oxygen atmosphere did not improve the yield. As despite suppressing the side reaction, TEMPO did not improve the yield of **2a**, we used TEMPO only for few substrates which produced significant amount of the ester product. In spite of having an acceptable synthetic condition in hand to produce 7-membered lactones, one of the major drawbacks of using super stoichiometric amount of peroxide remained an unsolved problem due to its explosive nature in the large-scale process development. Furthermore, formation of deleterious methyl ester **2a'** could be overcome if we succeed to eliminate DTBP. Intrigued by the captivating works on molecular oxygen by the Powers group (Maity et al., 2018a, 2018b), the Freakley group (Agarwal et al., 2017),

Table 1. Optimization of 7-membered lactone formation^{a,b}



Entry	Catalyst (20 mol%)	Oxidant	Solvent	Yield (%) 2a/2a'
1	CuI	DTBP (2.0 equiv)	DCE	52/25
2	CuI	DTBP (2.0 equiv)	PhCl	60/27
3	CuI	DTBP (2.0 equiv)	PhCF ₃	65/20
4	Cu(OAc) ₂	DTBP (2.0 equiv)	PhCF ₃	46/35
5	Cu(OTf) ₂	DTBP (2.0 equiv)	PhCF ₃	41/32
6	CuO	DTBP (2.0 equiv)	PhCF ₃	35/40
7	CuI	TBHP (2.0 equiv)	PhCF ₃	40/38
8	CuI	BPO (2.0 equiv)	PhCF ₃	20/0
9	CuI	TBPB (2.0 equiv)	PhCF ₃	38/20
10	CuNPs	DTBP (2.0 equiv)	PhCF ₃	80/18
11	Cu(0)	DTBP (2.0 eq)	PhCF ₃	82/12
12 ^c	Cu(0)	DTBP (2.0 equiv)	PhCF ₃	83/0
13 ^d	Cu(0)	DTBP (2.0 equiv)	PhCF ₃	69/0
14 ^e	Cu(0)	DTBP (2.0 equiv)	PhCF ₃	75/18
15 ^f	Cu(0)	DTBP (2.0 equiv)	PhCF ₃	56/27
16	Cu(0)	O ₂ (purged)	PhCF ₃	20/0
17 ^g	Cu(0)	O ₂ (purged)	PhCF ₃	20/0
18 ^h	Cu(0)	O ₂ (purged)	PhCF ₃	ND
19 ⁱ	Cu(0)	O ₂ (purged)	PhCF ₃	10/0
20 ^j	Cu(0)	O ₂ (purged)	PhCF ₃	Trace
21 ^k	Cu(0)	O ₂ (purged)	PhCF ₃	ND
22 ^l	Cu(0)	O ₂ (purged)	PhCF ₃	30/0
23 ^m	Cu(0)/EY	O ₂ (purged)	PhCF ₃	45/0
24 ^m	Cu(0)/RB	O ₂ (purged)	PhCF ₃	72/0
25 ^m	Cu(0)/Ru(bpy) ₃ Cl ₂	O ₂ (purged)	PhCF ₃	35/0
26 ^{l,m}	Cu(0)/RB	O ₂ (purged)	PhCF ₃	50/0

^aAll reactions were carried out in 0.2 mmol scale.

^bYields refer to here are overall isolated yields.

^cadditional amount of 2 equiv TEMPO.

^dadditional 2 equiv BHT.

^eunder Ar atmosphere.

^funder O₂ atmosphere.

^gadditional 30 mol% of Et₃N.

^hadditional 30 mol% of ethylenediamine.

ⁱadditional 30 mol% of pyridine.

^jadditional 30 mol% of Bpy.

^kadditional 30 mol% of terpyridine.

^ladditional 30 mol% of TMEDA was used.

^munder 32 W CFL.

and others (Sushkevich et al., 2017), we envisioned that the coupling of aerial oxygen as a terminal oxidant for this transformation would be synthetically sustainable and attractive. To investigate, a reaction of **1a** with catalytic copper powder under the oxygen atmosphere PhCF₃ afforded 20% of the desired product

(Entry 16, Table 1). The combination of an array of nitrogen-containing ligands did not improve the yield further (Entry 17–22, Table 1). Rueping and others have demonstrated the activation and utilization of molecular oxygen merging visible-light photoredox catalysis in metal-catalyzed C–H activations (Fabry and Rueping, 2016). In this line, we focused our attention to reoptimize the reaction condition under copper/photosensitizer dual catalytic condition. Simply purging the reaction vessel with oxygen and using 1 mol% Eosin Y (EY) furnished the desired product in 45% yield under white CFL (46 W) irradiation at 110°C (Entry 23, Table 1). Gratifyingly, the yield of the desired product was improved to 72% using 1 mol% Rose Bengal (RB) (Entry 24, Table 1) along with the unreacted substrate. Next, we proceeded to examine the substrate scope under this sustainable condition denoted as condition B and the corresponding yields are represented along with previous DTBP condition A.

Substrate scope

The requisite biaryl substrates bearing methyl and carboxylic acid at the 2,2'-position were prepared by Suzuki-Miyaura cross-coupling to examine the scope of this lactonization under these optimized conditions. Gratifyingly, a broad range of substrates underwent benzylic oxidation reaction to provide seven-membered lactones in moderate to good yields as shown in Scheme 2. Electron donating groups such as OMe, Me, OBn, and OEt on both rings A and B afforded moderate to good yields (2b–2g, 2m, 2q, 2r, 2v–2x, Scheme 2). Electron withdrawing groups such as NO₂, Cl, and F bearing substrates also provided moderate to a good yield of the product (2h–2l, 2n, 2p, 2s, 2z, 2aa, Scheme 2). Interestingly, besides methyl group, ethyl and aryl-substituted diarylmethanes also underwent seven-membered lactonization reaction chemo- and regioselectively (2l, 2o, 2t, 2y, 2aa, Scheme 2, Figure S2) which was a limitation in previous C–H activation methods (Dana et al., 2018; Zhang et al., 2015). Diarylmethanes (1t, 1y) provided better yields presumably due to activated benzylic C–H bond by two aryl groups. Notably, substrates bearing more than one methyl groups react at the *ortho* benzyl moiety leaving others intact (2b, 2e, 2i, 2k, 2m, 2n, 2q, 2w, Scheme 2). Hence, carboxylic acid might have a crucial role for intramolecular benzylic C–H activation to the formation of 7-membered lactone.

Attempt toward 8-membered lactone and serendipitous Smiles rearrangement

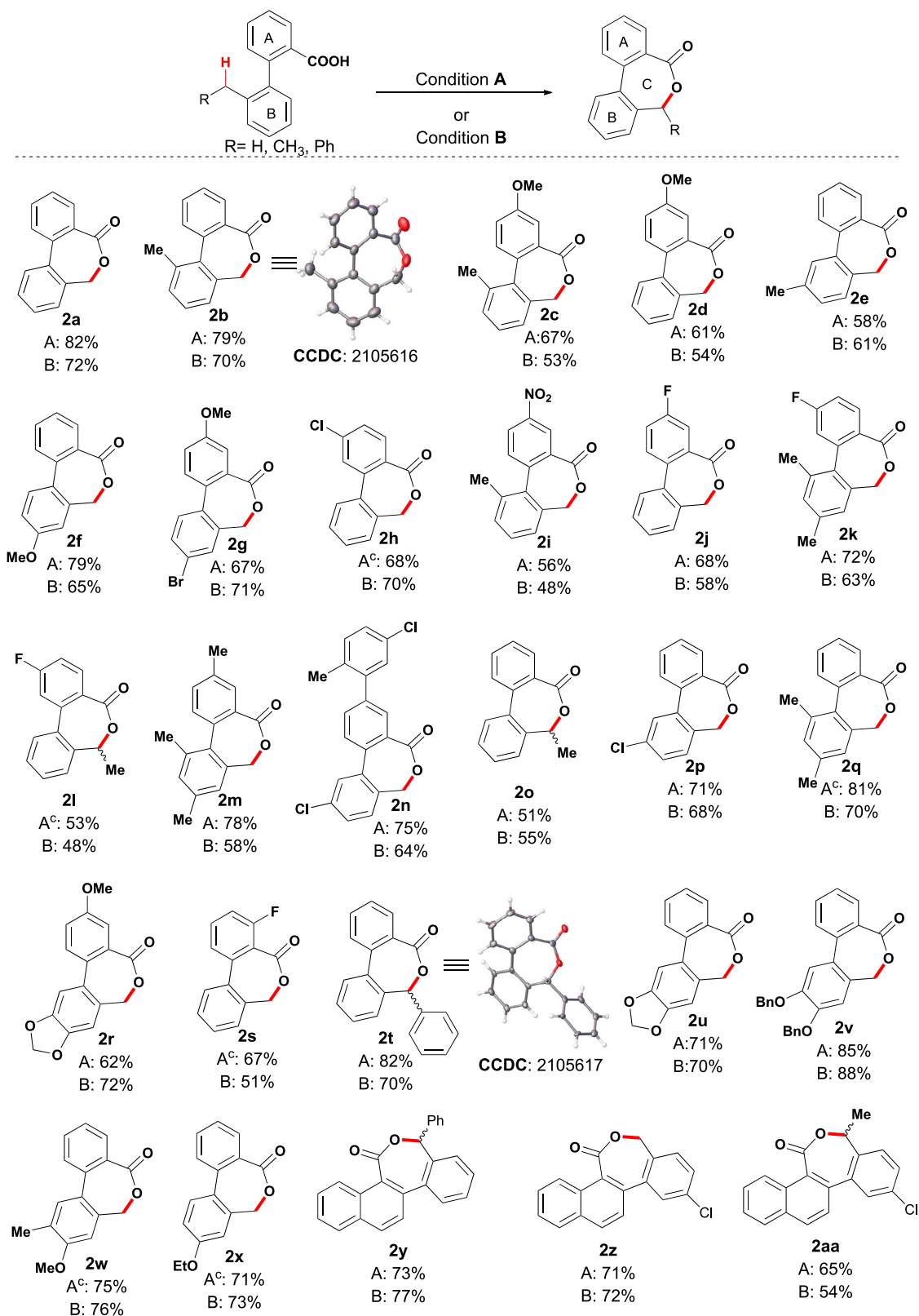
To examine the viability of the formation of 8-membered lactone, we prepared the corresponding diaryl ether 3a and subjected to the reaction condition A. Interestingly, instead of the expected product 4a', 2-hydroxyphenyl 2-methyl benzoate 4a was obtained in 62% yield through C–O bond cleavage and 1,5-aryl migration. The generation and involvement of carboxyl radical in this Smiles-type rearrangement has been reported by our group and others (Hossian and Jana, 2016; Wang et al., 2017). Subsequently, we examined the scope of 2-aryloxybenzoic acids with several substituents on both the phenol and aryl benzoic acid components, which provided moderate to good yields under the reaction condition (Scheme 3). The reaction was also reproduced in 0.5 mmol scale providing comparable yields which was a major limitation under our previous condition (4a, Scheme 3) (Hossian and Jana, 2016).

Double benzyl C–H activation en route to 7-membered lactone

We anticipated that the lactonization product can be obtained from 2,2'-alkyl biaryls by subtle tuning the reactivity between two alkyl moieties where one of them would be oxidized to the corresponding carboxylic acid. Therefore, 2,2'-dimethyl-1,1'-biphenyl (5a) was prepared and subjected to the reaction condition A. Gratifyingly, the desired 7-membered lactone 2a was obtained in 52% yield which is formed through 4-fold benzylic C–H bond cleavage. The yield was further improved to 65% on purging O₂. Besides unsubstituted benzyl, methyl- and phenyl-substituted substrates also furnished the desired product through the selective oxidation of methyl to carboxylic acid. Surprisingly, in case of unsymmetrical biaryls, the corresponding lactone products were obtained in moderate yields through the formation of carboxylic acid of CH₃, Cl, and OMe substituted-aryl methyls (Scheme 4). However, in case of 5d–f, an inseparable mixture presumably due to the lactonization from the other methyl group was observed resulting in lower isolated yields.

Synthetic utility: total synthesis of alterlactone

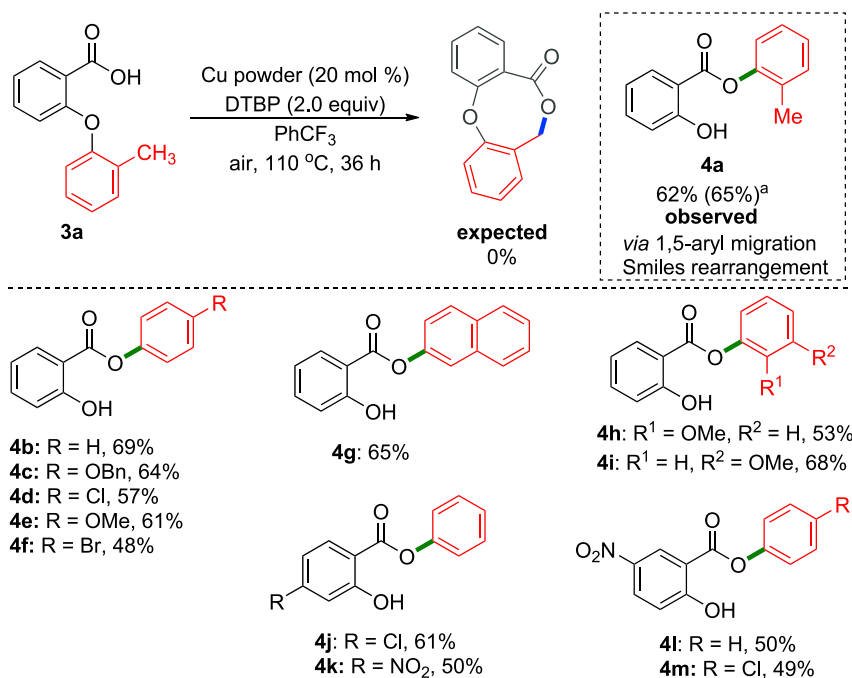
The synthetic utility of the present protocol was demonstrated through the total synthesis of a natural product alterlactone (Cudaj and Podlech, 2012) which was isolated from the extract of endophytic fungi *Alter-naria* sp. It is cytotoxic against L5178Y cells (Aly et al., 2008), neuroprotective, and Nrf2 activator in PC12



Scheme 2. Substrate scope of Dibenzo[c,e]oxepin-5(7H)-ones^{a,b}

Condition A: 20 mol% Cu, 2.0 equiv. DTBP, PhCF₃, 110 °C, air, 36–48 h. Condition B: 20 mol% Cu, 1 mol% Rose Bengal, PhCF₃, 110 °C, O₂, 32 W CFL, 36–48 h.

^aAll reactions were carried out in 0.2 mmol scale. ^bYields refer to the overall isolated yields. ^cAdditionally, 2.0 equiv TEMPO was used.



Scheme 3. Smiles rearrangement

20% Cu, 2 equiv DTBP, PhCF₃, 110 °C, air, 36 h. All reactions were carried out in 0.2 mmol scale. Yields refer to the overall isolated yields. ^ain 0.5 mmol scale.

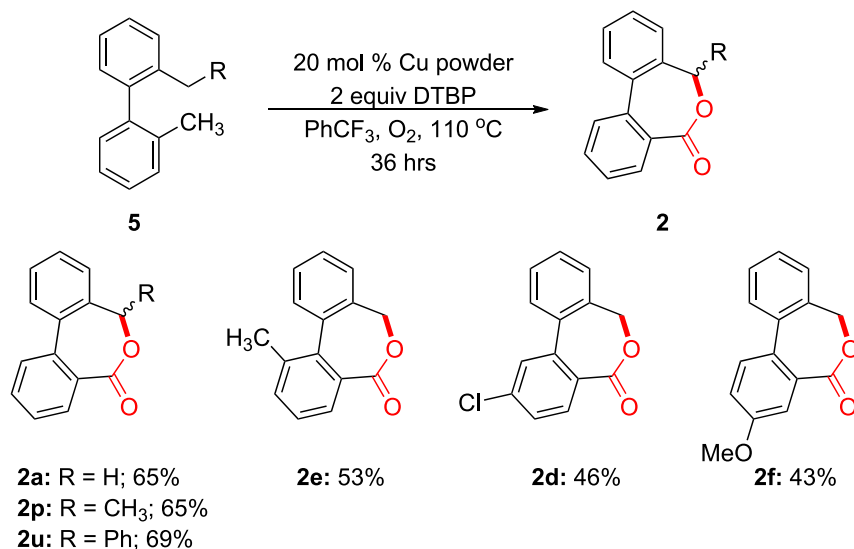
cells (Hou et al., 2021). We have successfully achieved the expected product alterlactone **18** in 10 steps starting from acetal-protected phloroglucinol acid and 3,4-hydroxytoluene (Scheme 5). In this total synthesis, we have applied our methodology at a late-stage under the dual catalytic condition which provided desired alterlactone after global deprotection of benzyl groups. This method is cost effective compared to the previous method (Cudaj and Podlech, 2012).

Practical demonstration and product derivatization

Furthermore, we hypothesized that the reaction might take place by itching the wall of copper vessel without any added copper catalyst. To our delight, the model substrate **2a** underwent the reaction smoothly under condition A in a 2.0 mmol scale furnishing 55% isolated yield of **3a** (Scheme 6A). Then, to check the scalability, model reaction was performed in 10 mmol scale under condition B. Gratifyingly, the reaction is reproducible furnishing 68% of the desired product **3a** (Scheme 6B). A thiolation reaction of dibenzo[*c,e*]joxepan-5-one **2a** with 0.5 equiv Lawesson's reagent afforded dibenzo[*c,e*]joxepan-5-thione **19** in 43% yield (Scheme 6C) which is an initiator for radical polymerization (Bingham and Roth, 2019). Finally, base hydrolysis of **2a** afforded the corresponding benzyl alcohol **20** in 92% yield (Scheme 6D).

Diverse reactivities with different substrates

To explore the suitability of the developed catalytic systems to differently designed substrates, a range of reactions were carried out (Schemes 7 and S1). Interestingly, in both the conditions, substrate **1ab**, which contains OH at the *para* and two CH₃ groups at two *ortho* positions of the second ring, underwent dearomatization to yield spiro lactone **24** instead of giving the eight-membered lactone. When indole **1af** was subjected to condition A, 6-membered lactone forms via C(sp²)-H activation and subsequent oxidation at C-3 position furnished dearomatized indole dione **25**. When benzyl alcohol substrate **26** was taken instead of benzoic acid, oxidation led to the formation of fluorenone **27** in lieu of the seven-membered lactone. Fascinatingly, the benzenesulfonamide **28** underwent the C(sp³)-H activation to yield the seven-membered lactam **29** under condition A. In our trial to expand the scope of eight-membered lactone formation (Chen et al., 2021), we took substrate **30**, which showed a different reactivity to afford five-membered lactone **31** selectively. Thus, a broad scope of diverse reactivities



Scheme 4. Lactonization through double benzylic C-H activation

Reaction condition: 20% Cu, 2 equiv DTBP, PhCF₃, 110 °C, O₂, 36 h. All reactions were carried out in 0.2 mmol scale. Yields refer to the overall isolated yields.

for the formation of seven- and five-membered lactonization via C–H could be opened up using this catalytic system.

Mechanistic study

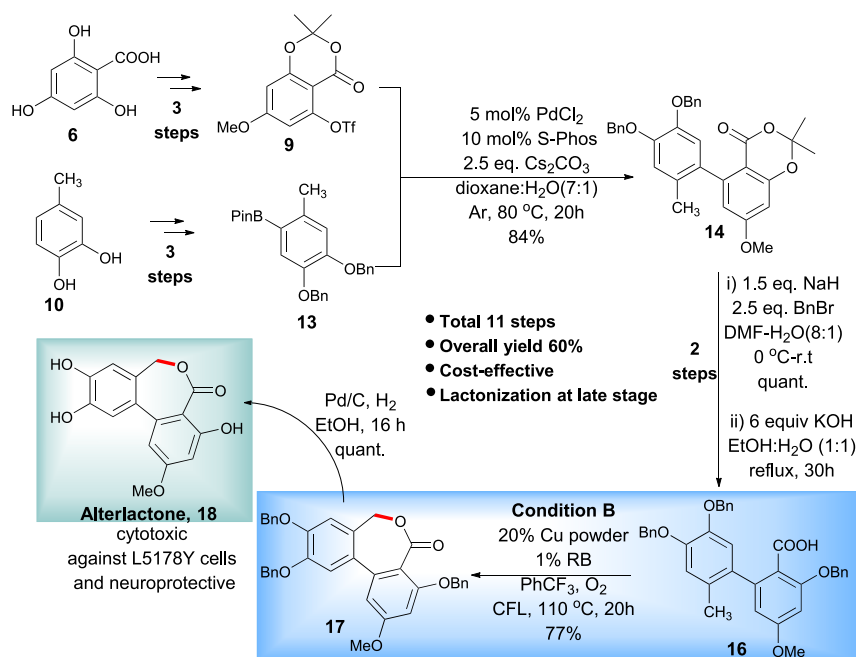
To elucidate the origin of high degree of chemoselectivity, we performed several control and spectroscopic experiments.

a) Radical quenching experiment

During optimization, we observed the formation of methyl ester **3a** by the methyl-radical which is formed through the decomposition of DTBP. This esterification was completely arrested by the addition of 2.0 equiv of TEMPO in the optimized reaction condition leading to the formation of a methyl radical adduct of TEMPO which was detected by the ESI-MS from an aliquot of reaction mixture (Scheme 8A(i)). After the complete suppression of 2.0 equiv methyl radical generated from 2.0 equiv DTBP, excess amount of TEMPO (e. g. 5.0 equiv) completely suppressed the formation of desired lactone **2a** and a TEMPO adduct with **1a** (M⁺–H) at benzylic or carboxylate (**22a** or **22a'**) position was detected in the ESI-MS (Schemes 8A(ii) and S10).

b) Competitive experiment between C(sp²)–H and C(sp³)–H activation

Interestingly, when **1a** was subjected to the Martin's reaction condition (Gallardo-Donaire and Martin, 2013), only the 6-membered lactone **23a** was obtained in 72% yield via C(sp²)–H activation selectively. On the other hand, in our optimized condition A and B, selectively 7-membered lactone **2a** was isolated in 82% and 72% yields, respectively (Scheme 8B). Besides energy difference (benzylic sp³ C–H vs sp² C–H bond; 85–90 vs 110–115 kcal/mol) (Blanksby and Ellison, 2003), the nature of oxidant cum radical initiator might have a crucial role for this chemoselectivity. From thorough control studies (Scheme S11), we observed that external oxidants capable of generating at least 1 equiv of methyl radicals e.g., DTBP, TBHP, and TBPB were effective. Hence, unlike the Martin's condition where BPO was effective oxidant for sp² C–H bond activation, was ineffective in our study. Presumably, the methyl radical generated through β-methyl scission of tert-butyl oxo radical might result in selective weak benzylic C–H bond cleavage and methane formation. Whereas, benzoyl radical or phenyl radical (via decarboxylation) generated *in situ* probably prefers sp² C–H bond activation. However, the origin of chemoselectivity in our developed peroxide-free condition B warrants further studies.



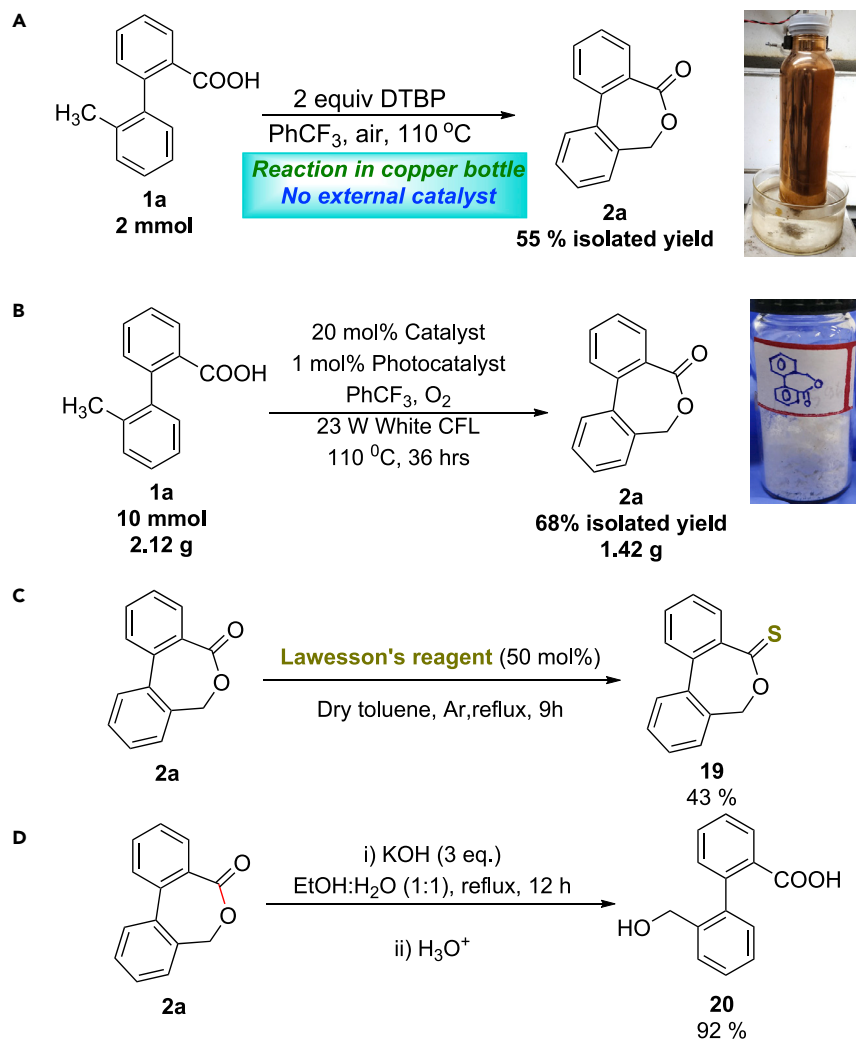
Scheme 5. Total synthesis of alterlactone

c) Addition of external substituted benzoic acids and ligands

To understand whether the reaction proceeds via inner- or outer-sphere copper complex, super stoichiometric (2.0 equiv) amount of benzoic acid was added to the reaction mixture under both conditions A and B. Surprisingly, no intermolecular benzoylation product was obtained except the desired lactonization products in moderate yields. Electron-rich 4-methoxy and electron-deficient 4-nitro benzoic acids also furnished similar results (Schemes 8C and S12). Furthermore, common external ligands such as pyridine, bipyridine, 1,10-phenanthroline, TMEDA etc. affected negatively in the reaction outcome (Scheme 8D) suggesting that copper might generate an inner sphere soluble complex binding with the substrate **1a** which was further supported by the spectroscopic studies.

d) UV and XPS studies of the reaction mixture

Because Cu(0) powder was used as an initial catalyst, we were intrigued to elucidate the formation of active catalyst and its oxidation state. Under the condition A (Figures 2A and S1) (Zhang et al., 2019), visually the insoluble Cu powder was converted to slightly suspended particles and showed light blue coloration after 6 h. Subsequently, it turned into an intense blue clear solution after 12 h indicating the formation of Cu(II) species. Finally, the solution turns into greenish color and turbid again. To check the presence of Cu(II) species unambiguously, UV-vis absorption spectra were recorded from the reaction mixture at 3 h interval. Notably, characteristic peak at 684 nm of Cu(II) appeared after 3 h with increasing intensity with the progress of the reaction (Figures 2B and S2) (Liang et al., 2020). No similar Cu(II) peak was observed in the absence of substrate and/or DTBP (Figures S3 and S4). It indicates that substrates may act as a ligand for the formation and stabilization of Cu(II) species. The UV-vis spectra from condition B also exhibited a similar spectral pattern indicating the formation of Cu(II) species to steer the reaction (Figures 2C and S5) where substrate was essential to stabilize the Cu(II) similarly (Figure S6). Notably, an intense peak of Cu(II) was observed just after 1 h using rose bengal/light (condition B) whereas a weak peak of the same appeared after 8 h without rose bengal/light (Figure S7). Hence, photoredox catalyst under light irradiation may accelerate the formation of active Cu(II) catalyst by molecular oxygen. However, the formation of Cu(III) species was not observed neither under condition A nor condition B. The oxidation state of the copper was further confirmed by XPS analysis. Under the condition B, the characteristic peaks at 931.0 and 950.9 eV are assigned to Cu 2p^{3/2} and 2p^{1/2} of Cu(II). An



Scheme 6. Practical demonstration and product derivatization

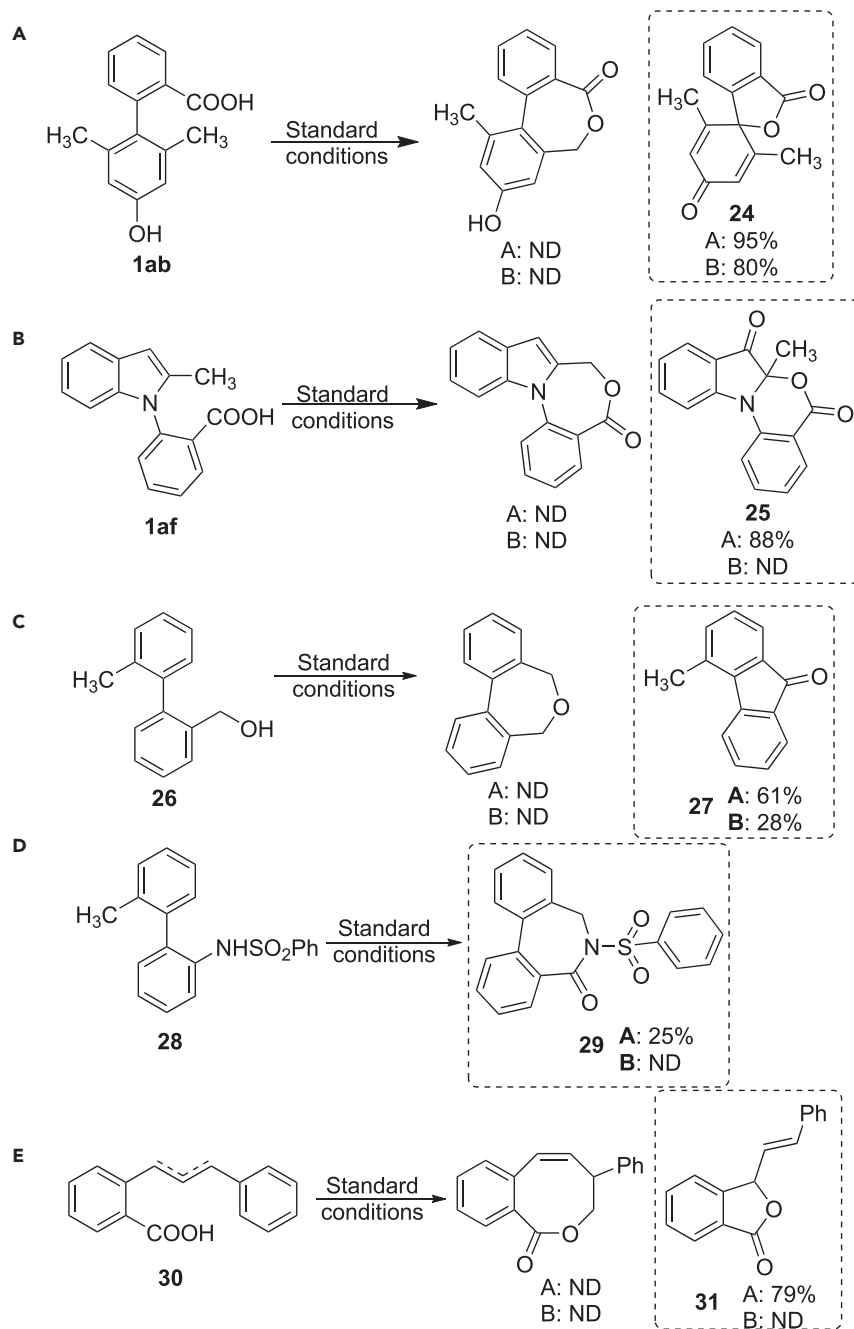
intense satellite peak at 942 eV confirms the presence of Cu(II) species in the reaction mixture (Figure 2D). (Maity et al., 2020) Similar peaks were also appeared in the condition A indicating the involvement of Cu(II) in this reaction (Figure S9).

e) Characterization of the recovered catalyst

Because an almost clear blue solution became turbid after the completion of the reaction (Figure S9), we assumed that copper (oxide or hydroxide) nanoparticles (CuNPs) might form. The transmission electron microscopic (TEM) image of both reaction mixtures indicated the formation of copper nanoparticles of 2–5 nm diameter (Figures 2E and S10). In fact, the reaction also took place using preformed nanoparticles (CuNPs), entry 10, Table 1. However, the size of the particles formed *in situ* from the copper powder may vary beyond the nanometer range.

Plausible mechanism

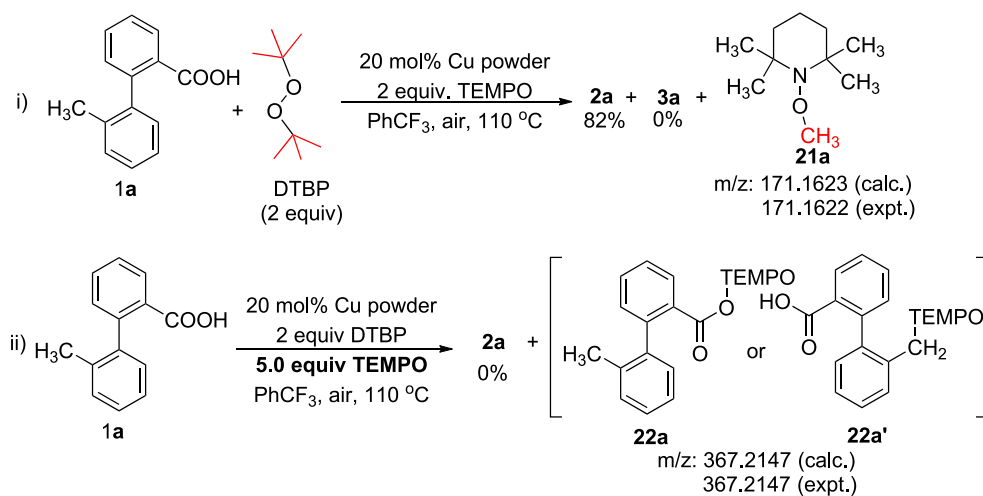
From the control and spectroscopic experiments, we envisioned the plausible mechanism as follows. Under condition A (Scheme 9), first DTBP undergoes homolytic cleavage followed by β -methyl scission to generate active methyl radical $\cdot\text{CH}_3$ and abstracts one proton from benzylic position of **1a** to emit CH_4 and corresponding benzylic radical species are formed. The evolution of CH_4 was

**Scheme 7. Diverse reactivities**

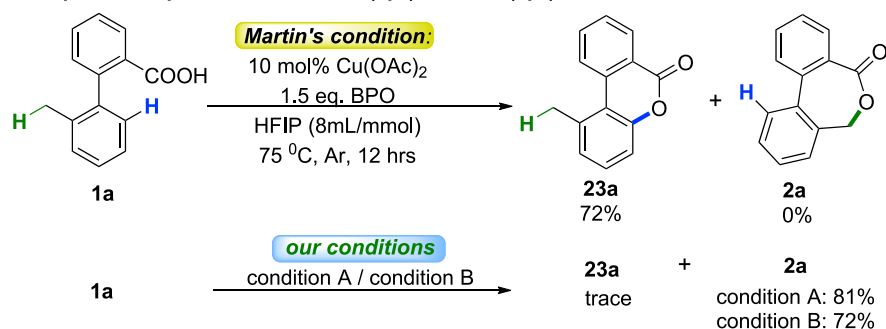
confirmed by gas chromatography of the sample taken from the reaction vessel (Figure S11). Subsequently, Cu(0) forms carboxylate to generate reactive intermediate I which readily gets stabilization by formation of 8-membered copper complex II. Thereafter, it undergoes reductive elimination to yield product 2a and regenerates Cu(0) which continues the reaction in forward direction. Besides, some amount of $\cdot\text{CH}_3$ is captured by the carboxyl group of the substrate to provide undesired 2a'.

Under condition B (Scheme 9), the benzylic C–H activation is believed to be performed by copper-peroxide radical formed from oxygen molecule via photosensitization. The RB is excited to RB^* upon

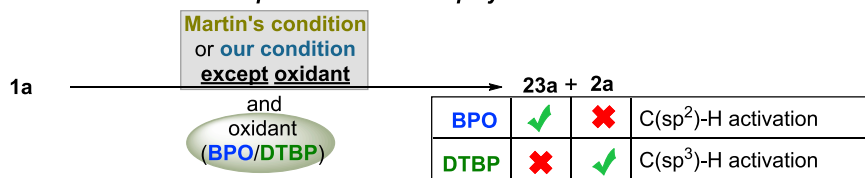
A TEMPO experiment



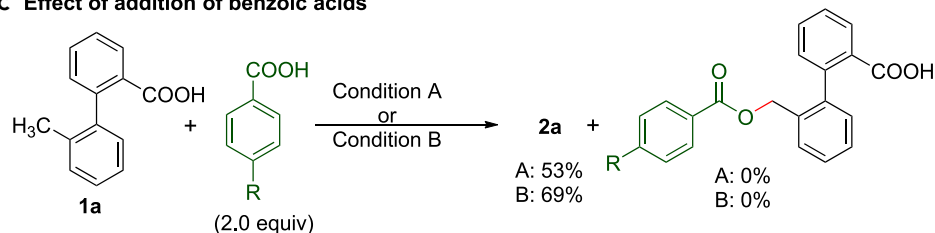
B Competitive experiment between C(sp²)-H and C(sp³)-H activation



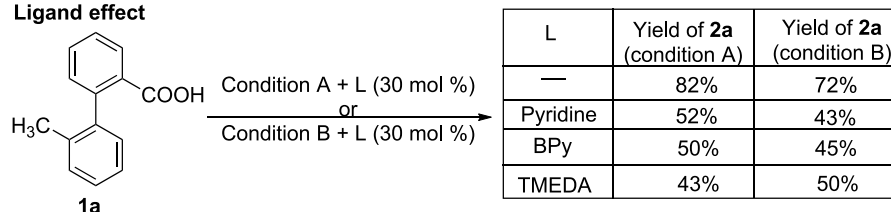
Result after series of control experiments: Oxidant plays the role



C Effect of addition of benzoic acids



D Ligand effect



Scheme 8. Control experiments

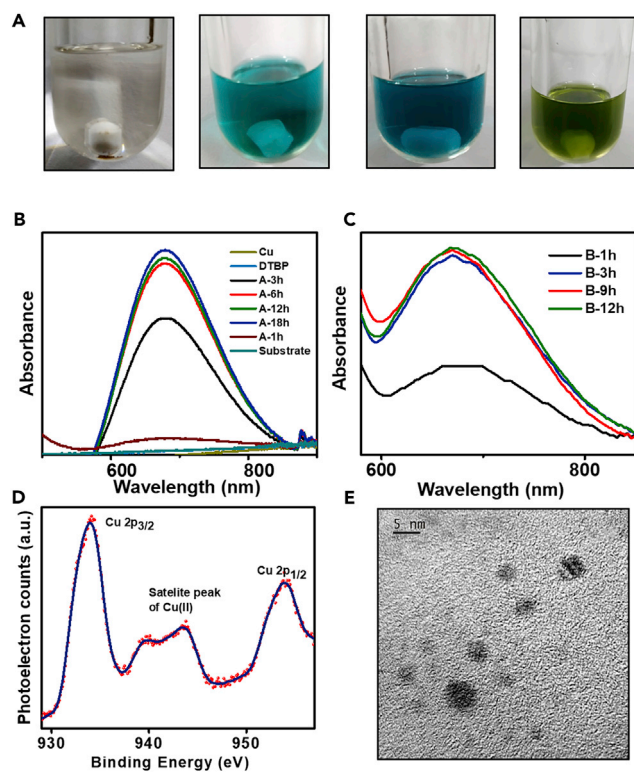
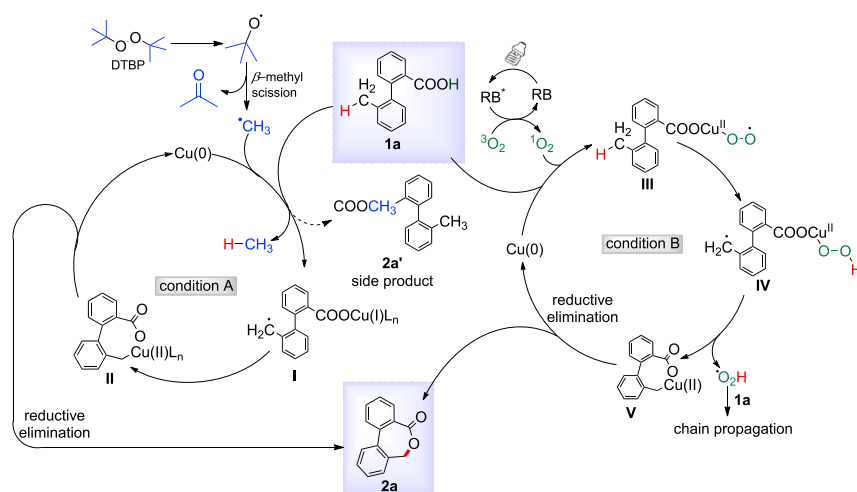


Figure 2. Mechanistic study

- (A) Digital photograph of *in situ* color change of standard reaction with condition A over time.
(B) UV-vis absorption spectra of standard reaction with condition A.
(C) *In situ* UV-vis absorption spectra of standard reaction with condition B.
(D) XPS analysis from condition B.
(E) TEM image of reaction mixture after 36 h from condition B.

irradiation of light and subsequently transfers energy to triplet oxygen ($^3\text{O}_2$) to produce singlet oxygen ($^1\text{O}_2$) (Wootton et al., 2002). Then, the Cu(0) scavenges the $^1\text{O}_2$ and reacts with carboxyl group (Hu et al., 2020b) of **1a** to generate copper(II)-peroxo intermediate (Davydov et al., 2022; Kunishita et al., 2008) **III** undergoing two simultaneous SET. Then, this copper-peroxo radical abstracts one proton from proximal benzylic position to produce benzylic radical intermediate **IV**. Subsequently, 8-membered Cu(II) complex **V** is formed while hydroperoxyl radical is released which may propagate the chain (Trammell et al., 2019) reacting with another molecule of **1a**. Complex **V** undergoes reductive elimination to furnish the final product **2a** and Cu(0) is regenerated. In either cases, copper-catalyzed initial oxidation of benzylic C–H bonds to benzyl alcohol followed by lactonization is plausible. However, neither by isolation nor via MS characterization, corresponding benzyl alcohol was identified from the reaction mixture. Furthermore, the corresponding benzyl alcohol **20**, which was obtained through hydrolysis of the lactonized product **2a**, converted back to lactone product **2a** in only 7% yield under our reaction condition (Scheme S13). Hence, initial benzylic oxidation to alcohol may not be a feasible pathway.

In the case of Scheme 4, one benzylic C(sp³)–H group of **5a** first oxidizes to the corresponding benzoic acid **2a** under the highly oxidative condition (Mohammadpour and Safaei, 2020; Sutradhar et al., 2017) and then follows the mechanism corresponding to the condition A to afford the product **2a** (Scheme S14). Notably, when there is one 2° and another 1° benzylic C(sp³)–H groups in the substrates (**5p**, **5u**), the 1° benzylic C–H (i.e. CH₃ group) first oxidizes to benzoic acid followed by the activation of 2° benzylic C–H activation and subsequent cyclization to achieve the products. And, when any substitution is present in either ring (**5d-f**), the controlling factor of sequence of oxidation and activation of the two benzylic C(sp³)–H groups demand further investigations.



Scheme 9. Plausible mechanism

Recyclability of the catalysts

Fortunately, a metallic precipitation was appeared after the completion of the reaction. Hence, we intended to recover and reuse the catalyst to enhance the practical utility (Pla and Gómez, 2016). After a batch reaction, the catalyst was recovered by simple filtration, washed with ethyl acetate, and subjected to the subsequent batch of reaction. Delightedly, 75% of our desired product 2a was isolated in the second run. Similarly, a total of subsequent four batches of the same reaction were repeated without further addition of Cu catalyst furnishing 82%, 75%, 66%, and 48% yields, respectively (Figure 3). Similarly, the catalysts including rose bengal were also recycled and reused in the Cu/O₂ system (Condition B) as depicted in Figure 3. Washing the precipitate with organic solvents (Chen et al., 2006) or acetic acid (Argyle and Bartholomew, 2015) to further enhance the catalytic activity went in vain. Still, this is rare and exciting example where inexpensive copper powder is converted to the substrate-bound homogeneous catalyst for highly chemoselective benzylic oxidation and finally, precipitate out facilitating catalyst recovery.

Conclusion

We disclosed here an inexpensive copper powder-catalyzed chemoselective benzylic sp³ C–H activation for the direct synthesis of seven-membered dibenzo[c,e]oxepin-5(7H)-ones. Remarkably, hazardous oxidant di-tert-butyl peroxide (DTBP) was replaced by molecular oxygen merging with organic photosensitizer. Interestingly, a highly reactive, substrate-dependent soluble catalyst is formed from the copper powder during the reaction to achieve a high degree of chemoselective benzylic sp³ C–H oxidation suppressing the six-membered lactone formation via the sp² C–H bond activation. Finally, the heterogeneous catalyst is precipitated out and recovered for subsequent runs by simple filtration offering maximum benefits of homo- and heterogeneous catalyst. The reaction proceeds through a single electron transfer (SET)

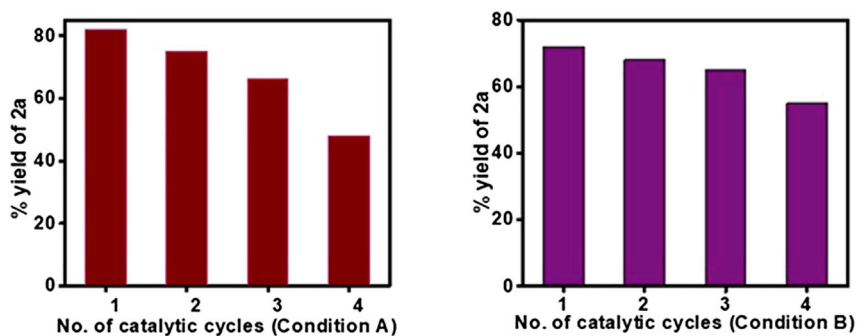


Figure 3. Recyclability of the catalysts

pathway, is scalable and applied to the total synthesis of cytotoxic natural product alterlactone. Further exploration of Cu(0)/photoredox/O₂ is undergoing in our laboratory.

Limitations of the study

Despite advantageous development of sustainable conditions for benzylic C(sp³)-H activation toward lactone formation, it is limited to 7-membered lactones. The substrate class **3** furnished Smiles rearrangement product via 1,5-aryl migration instead of 8-membered lactone formation. Aldehyde, primary amines were incompatible under the reaction conditions. Recovered catalyst was found to be inferior in catalytic efficiency after four runs, which could be a subject of further improvement.

STAR★METHODS

Detailed methods are provided in the online version of this paper and include the following:

- KEY RESOURCES TABLE
- RESOURCE AVAILABILITY
 - Lead contact
 - Materials availability
 - Data and code availability
- METHOD DETAILS
 - General reagent information
 - General analytical information
 - General procedure for preparation of starting materials 2'-alkyl-[1,1'-biphenyl]-2-carboxylic acids (1)
 - General experimental procedure for the preparation of 2-aryloxybenzoic acids (3)
 - Preparation of starting materials 2-alkyl-2'-methyl-1,1'-biphenyls (5)
 - Reaction profile of the standard reaction under condition A and B (Scheme 2)
 - General experimental procedure for the carboxyl radical assisted 1,5-aryl migration through Smiles rearrangement using 2-phenoxybenzoic acids, Scheme 4
 - General experimental procedures for copper-catalyzed chemo- and regioselective double C-H activation of 2-alkyl-2'-methyl-1,1'-biphenyls (5), Scheme 5
 - Experimental procedure for total synthesis of alterlactone (21)
 - Derivatization procedures
 - Practical demonstrations
 - Spectroscopic details

SUPPLEMENTAL INFORMATION

Supplemental information can be found online at <https://doi.org/10.1016/j.isci.2022.104341>.

ACKNOWLEDGMENTS

This work was supported by DST, SERB, Govt. of India Core Research Grant No. CRG/2021/006717. S.N. and S.M. thank DST and CSIR for their respective fellowships.

AUTHOR CONTRIBUTIONS

R.J. and S.N. envisioned and designed the project and wrote the manuscript. S.N. and S.M. conducted the methodology development, synthesis, and characterization of compounds. R.J. supervised the project overall.

DECLARATION OF INTERESTS

The authors declare no competing interests.

Received: January 20, 2022

Revised: April 9, 2022

Accepted: April 26, 2022

Published: May 20, 2022

REFERENCES

- Agarwal, N., Freakley, S.J., McVicker, R.U., Althabhan, S.M., Dimitratos, N., He, Q., Morgan, D.J., Jenkins, R.L., Willock, D.J., Taylor, S.H., et al. (2017). Aqueous Au-Pd colloids catalyze selective CH₄ oxidation to CH₃OH with O₂ under mild conditions. *Science* 358, 223–227. <https://doi.org/10.1126/science.aan6515>.
- Altemöller, M., Gehring, T., Cudaj, J., Podlech, J., Goesmann, H., Feldmann, C., and Rothenberger, A. (2009). Total synthesis of graphisrhone A, C, D, and H, of ulocladol, and of the originally proposed and revised structures of graphisrhone E and F. *Eur. J. Org. Chem.* 2009, 2130–2140. <https://doi.org/10.1002/ejoc.200801278>.
- Aly, A.H., Edrada-Ebel, R., Indriani, I.D., Wray, V., Müller, W.E.G., Totzke, F., Zirrgiebel, U., Schächtele, C., Kubbutat, M.H.G., Lin, W.H., and Proksch, P. (2008). Cytotoxic metabolites from the fungal endophyte *Alternaria* sp. and their subsequent detection in its host plant *Polygonum senegalense*. *J. Nat. Prod.* 71, 972–980. <https://doi.org/10.1021/np070447m>.
- Aneja, T., Neetha, M., Afsina, C.M.A., and Anilkumar, G. (2020). Progress and prospects in copper-catalyzed C–H functionalization. *RSC Adv.* 10, 34429–34458. <https://doi.org/10.1039/d0ra06518h>.
- Argyle, M.D., and Bartholomew, C.H. (2015). Heterogeneous catalyst deactivation and regeneration: a review. *Catalysts* 5, 145–269. <https://doi.org/10.3390/catal5010145>.
- Barzanò, G., Mao, R., Garreau, M., Waser, J., and Hu, X. (2020). Tandem photoredox and copper-catalyzed decarboxylative C(sp³)–N coupling of anilines and imines using an organic photocatalyst. *Org. Lett.* 22, 5412–5416. <https://doi.org/10.1021/acs.orglett.0c01769>.
- Bhunia, S.K., Das, P., Nandi, S., and Jana, R. (2019). Carboxylation of aryl triflates with CO₂ merging palladium and visible-light-photoredox catalysts. *Org. Lett.* 21, 4632–4637. <https://doi.org/10.1021/acs.orglett.9b01532>.
- Bingham, N.M., and Roth, P.J. (2019). Degradable vinyl copolymers through thiocarbonyl addition–ring-opening (TARO) polymerization. *Chem. Commun.* 55, 55–58. <https://doi.org/10.1039/c8cc08287a>.
- Blanksby, S.J., and Ellison, G.B. (2003). Bond dissociation energies of organic molecules. *Acc. Chem. Res.* 36, 255–263. <https://doi.org/10.1002/chin.200324299>.
- Carrillo-Arcos, U.A., Rojas-Ocampo, J., and Porcel, S. (2016). Oxidative cyclization of alkenoic acids promoted by AgOAc. *Dalton Trans.* 45, 479–483. <https://doi.org/10.1039/c5dt03808a>.
- Chen, C.-X., Xu, C.-H., Feng, L.-R., Qiu, F.-L., and Suo, J.-S. (2006). Deactivation and reactivation of copper-containing pentatomic hydroxalate in catalytic hydroxylation of phenol. *J. Mol. Catal. A. Chem.* 252, 171–175. <https://doi.org/10.1016/j.molcata.2006.01.065>.
- Chen, S., Mu, D., Mai, P.-L., Ke, J., Li, Y., and He, C. (2021). Enantioselective construction of six- and seven-membered triorgano-substituted silicon-stereogenic heterocycles. *Nat. Commun.* 12, 1249. <https://doi.org/10.1038/s41467-021-21489-6>.
- Chi, H., Li, H., Liu, B., Ye, R., Wang, H., Guo, Y.-L., Tan, Q., and Xu, B. (2019). From isocyanides to iminonitriles via silver-mediated sequential insertion of C(sp³)–H bond. *iScience* 21, 650–663. <https://doi.org/10.1016/j.isci.2019.10.057>.
- Cianfanelli, M., Olivo, G., Milan, M., Klein Gebbink, R.J.M., Ribas, X., Bietti, M., and Costas, M. (2020). Enantioselective C–H lactonization of unactivated methylenes directed by carboxylic acids. *J. Am. Chem. Soc.* 142, 1584–1593. <https://doi.org/10.1021/jacs.9b12239>.
- Colombel, V., Joncour, A., Thoret, S., Dubois, J., Bignon, J., Wdziczak-Bakala, J., and Baudoin, O. (2010). Synthesis of antimicrotubule dibenzoxepines. *Tetrahedron Lett.* 51, 3127–3129. <https://doi.org/10.1016/j.tetlet.2010.04.039>.
- Copéret, C., Chabanas, M., Saint-Arroman, R.P., and Basset, J.-M. (2003). Homogeneous and heterogeneous catalysis: bridging the gap through surface organometallic chemistry. *Angew. Chem. Int. Ed.* 42, 156–181. <https://doi.org/10.1002/chin.200316246>.
- Cudaj, J., and Podlech, J. (2012). Total synthesis of altenuin and alterlactone. *Synlett* 23, 371–374. <https://doi.org/10.1055/s-0031-1290135>.
- Cui, X., Li, W., Ryabchuk, P., Junge, K., and Beller, M. (2018). Bridging homogeneous and heterogeneous catalysis by heterogeneous single-metal-site catalysts. *Nat. Catal.* 1, 385–397. <https://doi.org/10.1038/s41929-018-0090-9>.
- Curto, J.M., and Kozłowski, M.C. (2015). Chemoselective activation of sp³ vs sp² C–H bonds with Pd(II). *J. Am. Chem. Soc.* 137, 18–21. <https://doi.org/10.1021/ja5093166>.
- Dai, J.-J., Xu, W.-T., Wu, Y.-D., Zhang, W.-M., Gong, Y., He, X.-P., Zhang, X.-Q., and Xu, H.-J. (2015). Silver-catalyzed C(sp²)–H functionalization/C–O cyclization reaction at room temperature. *J. Org. Chem.* 80, 911–919. <https://doi.org/10.1021/jo5024238>.
- Dalton, T., Faber, T., and Glorius, F. (2021). C–H activation: toward sustainability and applications. *ACS Cent. Sci.* 7, 245–261. <https://doi.org/10.1021/acscentsci.0c01413>.
- Dana, S., Chowdhury, D., Mandal, A., Chipem, F.A.S., and Baidya, M. (2018). Ruthenium(II) catalysis/noncovalent interaction synergy for cross-dehydrogenative coupling of arene carboxylic acids. *ACS Catal.* 8, 10173–10179. <https://doi.org/10.1021/acscatal.8b03392>.
- Das, J., Dolui, P., Ali, W., Biswas, J.P., Chandrashekar, H.B., Prakash, G., and Maiti, D. (2020). A direct route to six and seven membered lactones via γ -C(sp³)–H activation: a simple protocol to build molecular complexity. *Chem. Sci.* 11, 9697–9702. <https://doi.org/10.1039/d0sc03144e>.
- Davydov, R., Herzog, A.E., Jodts, R.J., Karlin, K.D., and Hoffman, B.M. (2022). End-on copper(I) superoxo and Cu(II) peroxo and hydroperoxo complexes generated by cryoreduction/annealing and characterized by EPR/ENDOR spectroscopy. *J. Am. Chem. Soc.* 144, 377–389. <https://doi.org/10.1021/jacs.1c10252>.
- Fabry, D.C., and Rueping, M. (2016). Merging visible light photoredox catalysis with metal catalyzed C–H activations: on the role of oxygen and superoxide ions as oxidants. *Acc. Chem. Res.* 49, 1969–1979. <https://doi.org/10.1021/acs.accounts.6b00275>.
- Feng, J., Liang, S., Chen, S.-Y., Zhang, J., Fu, S.-S., and Yu, X.-Q. (2012). A metal-free oxidative esterification of the benzyl C–H bond. *Adv. Synth. Catal.* 354, 1287–1292. <https://doi.org/10.1002/adsc.201100920>.
- Fukuyama, T., Maetani, S., Miyagawa, K., and Ryu, I. (2014). Synthesis of fluorenones through rhodium-catalyzed intramolecular acylation of biarylcarboxylic acids. *Org. Lett.* 16, 3216–3219. <https://doi.org/10.1021/ol5012407>.
- Gallardo-Donaire, J., and Martin, R. (2013). Cu-Catalyzed Mild C(sp³)–H Functionalization Assisted by Carboxylic Acids en Route to Hydroxylated Arenes. *J. Am. Chem. Soc.* 135, 9350–9353. <https://doi.org/10.1021/ja4047894>.
- Gandeepan, P., Müller, T., Zell, D., Cera, G., Warratz, S., and Ackermann, L. (2019). 3d transition metals for C–H activation. *Chem. Rev.* 119, 2192–2452. <https://doi.org/10.1021/acs.chemrev.8b00507>.
- Guo, S., Yuan, Y., and Xiang, J. (2015a). Copper-catalyzed oxidative alkenylation of C(sp³)–H bonds via benzyl or alkyl radical addition to β -nitrostyrenes. *New J. Chem.* 39, 3093–3097. <https://doi.org/10.1039/c4nj02416h>.
- Guo, X.-X., Gu, D.-W., Wu, Z., and Zhang, W. (2015b). Copper-catalyzed C–H functionalization reactions: efficient synthesis of heterocycles. *Chem. Rev.* 115, 1622–1651. <https://doi.org/10.1021/cr500410y>.
- Höller, U., Wright, A.D., Mathee, G.F., König, G.M., Draeger, S., Aust, H.-J., and Schulz, B. (2000). Fungi from marine sponges: diversity, biological activity and secondary metabolites. *Mycol. Res.* 104, 1354–1365. <https://doi.org/10.1017/s0953756200003117>.
- Hong, G., Nahide, P.D., Kumar Neelam, U., Amadeo, P., Vijeta, A., Curto, J.M., Hendrick, C.E., VanGelder, K.F., and Kozłowski, M.C. (2019). Palladium-catalyzed chemoselective activation of sp³ vs sp² C–H bonds: oxidative coupling to form quaternary centers. *ACS Catal.* 9, 3716–3724. <https://doi.org/10.1021/acscatal.9b00091>.
- Hossian, A., and Jana, R. (2016). Carboxyl radical-assisted 1,5-aryl migration through Smiles rearrangement. *Org. Biomol. Chem.* 14, 9768–9779. <https://doi.org/10.1039/c6ob01758d>.
- Hou, Y., Li, J., Wu, J.-C., Wu, Q.-X., and Fang, J. (2021). Activation of cellular antioxidant defense system by naturally occurring dibenzopyrone derivatives confers neuroprotection against oxidative insults. *ACS Chem. Neurosci.* 12, 2798–2809. <https://doi.org/10.1021/acchemneuro.1c00023>.
- Hu, H., Chen, S.-J., Mandal, M., Pratik, S.M., Buss, J.A., Krška, S.W., Cramer, C.J., and Stahl, S.S. (2020a). Copper-catalyzed benzylic C–H coupling

- with alcohols via radical relay enabled by redox buffering. *Nat. Catal.* 3, 358–367. <https://doi.org/10.1038/s41929-020-0425-1>.
- Hu, X.-Q., Liu, Z.-K., Hou, Y.-X., and Gao, Y. (2020b). Single electron activation of aryl carboxylic acids. *iScience* 23, 101266. <https://doi.org/10.1016/j.isci.2020.101266>.
- Ju, L., Yao, J., Wu, Z., Liu, Z., and Zhang, Y. (2013). Palladium-catalyzed oxidative acetoxylation of benzylic C–H bond using bidentate auxiliary. *J. Org. Chem.* 78, 10821–10831. <https://doi.org/10.1021/jo401830k>.
- Khake, S.M., and Chatani, N. (2020). Nickel-catalyzed C–H functionalization using A non-directed strategy. *Chem* 6, 1056–1081. <https://doi.org/10.1016/j.chempr.2020.04.005>.
- Krätschmar, F., Kaßel, M., Delony, D., and Breder, A. (2015). Selenium-catalyzed C(sp³)–H acyloxylation: application in the expedient synthesis of isobenzofuranones. *Chem. Eur. J.* 21, 7030–7034. <https://doi.org/10.1002/chem.201406290>.
- Kunishita, A., Ishimaru, H., Nakashima, S., Ogura, T., and Itoh, S. (2008). Reactivity of mononuclear alkylperoxo copper(II) complex. O–O bond cleavage and C–H bond activation. *J. Am. Chem. Soc.* 130, 4244–4245. <https://doi.org/10.1021/ja800443s>.
- Lerchen, A., Knecht, T., Koy, M., Ernst, J.B., Bergander, K., Daniliuc, C.G., and Glorius, F. (2018). Non-directed cross-dehydrogenative (Hetero)arylation of allylic C(sp³)–H bonds enabled by C–H activation. *Angew. Chem. Int. Ed.* 57, 15248–15252. <https://doi.org/10.1002/anie.201807047>.
- Li, Y., Ding, Y.-J., Wang, J.-Y., Su, Y.-M., and Wang, X.-S. (2013). Pd-catalyzed C–H lactonization for expedient synthesis of biaryl lactones and total synthesis of cannabiol. *Org. Lett.* 15, 2574–2577. <https://doi.org/10.1021/ol400877q>.
- Li, L., Yang, Q., Jia, Z., and Luo, S. (2018). Organocatalytic electrochemical C–H lactonization of aromatic carboxylic acids. *Synthesis* 50, 2924–2929. <https://doi.org/10.1055/s-0036-1591558>.
- Li, H., Subbotina, E., Bunrit, A., Wang, F., and Samec, J.S.M. (2019). Functionalized spirolactones by photoinduced dearomatization of biaryl compounds. *Chem. Sci.* 10, 3681–3686. <https://doi.org/10.1039/c8sc05476b>.
- Liang, T., Zhao, H., Gong, L., Jiang, H., and Zhang, M. (2019). Synthesis of multisubstituted benzimidazolones via copper-catalyzed oxidative tandem C–H aminations and alkyl deconstructive carbonyl functionalization. *iScience* 15, 127–135. <https://doi.org/10.1016/j.isci.2019.04.019>.
- Liang, Q., Walsh, P.J., and Jia, T. (2020). Copper-catalyzed intermolecular difunctionalization of styrenes with thiosulfonates and arylboronic acids via a radical relay pathway. *ACS Catal.* 10, 2633–2639. <https://doi.org/10.1021/acscatal.9b04887>.
- Liu, L., and Corma, A. (2018). Metal catalysts for heterogeneous catalysis: from single atoms to nanoclusters and nanoparticles. *Chem. Rev.* 118, 4981–5079. <https://doi.org/10.1021/acs.chemrev.7b00776>.
- Liu, S., Achou, R., Boulanger, C., Pawar, G., Kumar, N., Lusseau, J., Robert, F., and Landais, Y. (2020). Copper-catalyzed oxidative benzylic C(sp³)–H amination: direct synthesis of benzylic carbamates. *Chem. Commun.* 56, 13013–13016. <https://doi.org/10.1039/d0cc05226d>.
- Lu, B., Zhu, F., Sun, H.-M., and Shen, Q. (2017). Esterification of the primary benzylic C–H bonds with carboxylic acids catalyzed by ionic iron(III) complexes containing an imidazolium cation. *Org. Lett.* 19, 1132–1135. <https://doi.org/10.1021/acs.orglett.7b00148>.
- Maity, A., Hyun, S.-M., and Powers, D.C. (2018a). Oxidase catalysis via aerobically generated hypervalent iodine intermediates. *Nat. Chem.* 10, 200–204. <https://doi.org/10.1038/nchem.2873>.
- Maity, A., Hyun, S.-M., Wortman, A.K., and Powers, D.C. (2018b). Oxidation catalysis by an aerobically generated dess–martin periodinane analogue. *Angew. Chem. Int. Ed.* 57, 7205–7209. <https://doi.org/10.1002/ange.201804159>.
- Maity, S., Bain, D., Chakraborty, S., Kolay, S., and Patra, A. (2020). Copper nanocluster (Cu₂₃ NC)-Based biomimetic system with peroxidase activity. *ACS Sustainable Chem. Eng.* 8, 18335–18344. <https://doi.org/10.1021/acssuschemeng.0c07431>.
- Meng, H., Xu, Z., Qu, Z., Huang, H., and Deng, G.-J. (2020). Copper(0)/PPh₃-Mediated bisheteroannulations of o-nitroalkynes with methylketoximes accessing pyrazo-fused pseudoindoxyls. *Org. Lett.* 22, 6117–6121. <https://doi.org/10.1021/acs.orglett.0c02180>.
- Miyagawa, M., and Akiyama, T. (2018). Tishchenko reaction using substoichiometric amount of metallic Zinc. *Chem. Lett.* 47, 78–81. <https://doi.org/10.1246/cl.170897>.
- Mohammadpour, P., and Safaei, E. (2020). Catalytic C–H aerobic and oxidant-induced oxidation of alkylbenzenes (including toluene derivatives) over VO₂⁺ immobilized on core-shell Fe₃O₄@SiO₂ at room temperature in water. *RSC Adv.* 10, 23543–23553. <https://doi.org/10.1039/d0ra03483e>.
- Omura, S., Fukuyama, T., Murakami, Y., Okamoto, H., and Ryu, I. (2009). Hydrooruthenation triggered catalytic conversion of dialdehydes and keto aldehydes to lactones. *Chem. Commun.* 6741–6743. <https://doi.org/10.1039/b912850f>.
- Pla, D., and Gómez, M. (2016). Metal and metal oxide nanoparticles: a lever for C–H functionalization. *ACS Catal.* 6, 3537–3552. <https://doi.org/10.1021/acscatal.6b00684>.
- Ramirez, N.P., Bosque, I., and Gonzalez-Gomez, J.C. (2015). Photocatalytic dehydrogenative lactonization of 2-arylbenzoic acids. *Org. Lett.* 17, 4550–4553. <https://doi.org/10.1021/acs.orglett.5b02269>.
- Rout, S.K., Guin, S., Ghara, K.K., Banerjee, A., and Patel, B.K. (2012). Copper catalyzed oxidative esterification of aldehydes with alkylbenzenes via cross dehydrogenative coupling. *Org. Lett.* 14, 3982–3985. <https://doi.org/10.1021/ol301756y>.
- Rout, S.K., Guin, S., Ali, W., Gogoi, A., and Patel, B.K. (2014). Copper-catalyzed esterification of alkylbenzenes with cyclic ethers and cycloalkanes via C(sp³)–H activation following cross-dehydrogenative coupling. *Org. Lett.* 16, 3086–3089. <https://doi.org/10.1021/ol5011906>.
- Sathyamoorthi, S., and Du Bois, J. (2016). Copper-catalyzed oxidative cyclization of carboxylic acids. *Org. Lett.* 18, 6308–6311. <https://doi.org/10.1021/acs.orglett.6b03176>.
- Shao, A., Zhan, J., Li, N., Chiang, C.-W., and Lei, A. (2018). External oxidant-free dehydrogenative lactonization of 2-arylbenzoic acids via visible-light photocatalysis. *J. Org. Chem.* 83, 3582–3589. <https://doi.org/10.1021/acs.joc.7b03195>.
- Shi, Y., Zhang, T., Jiang, X.-M., Xu, G., He, C., and Duan, C. (2020). Synergistic photoredox and copper catalysis by diode-like coordination polymer with twisted and polar copper–dye conjugation. *Nat. Commun.* 11, 5384. <https://doi.org/10.1038/s41467-020-19172-3>.
- Sushkevich, V.L., Palagin, D., Ranocchiaro, M., and van Bokhoven, J.A. (2017). Selective anaerobic oxidation of methane enables direct synthesis of methanol. *Science* 356, 523–527. <https://doi.org/10.1126/science.aam9035>.
- Sutradhar, M., Alegria, E.C.B.A., Roy Barman, T., Scorzellotti, F., Guedes da Silva, M.F.C., and Pombeiro, A.J.L. (2017). Microwave-assisted peroxidative oxidation of toluene and 1-phenylethanol with monomeric keto and polymeric enol aroylhydrazone Cu(II) complexes. *Mol. Catal.* 439, 224–232. <https://doi.org/10.1016/j.mcat.2017.07.006>.
- Tang, P.-T., Shao, Y.-X., Wang, L.-N., Wei, Y., Li, M., Zhang, N.-J., Luo, X.-P., Ke, Z., Liu, Y.-J., and Zeng, M.-H. (2020a). Synthesis of seven-membered lactones by regioselective and stereoselective iodolactonization of electron-deficient olefins. *Chem. Commun.* 56, 6680–6683. <https://doi.org/10.1039/c9cc10080f>.
- Tang, Y., Meador, R.I.L., Malinchak, C.T., Harrison, E.E., McCaskey, K.A., Hempel, M.C., and Funk, T.W. (2020b). (Cyclopentadienone) iron-catalyzed transfer dehydrogenation of symmetrical and unsymmetrical diols to lactones. *J. Org. Chem.* 85, 1823–1834. <https://doi.org/10.1021/acs.joc.9b01884>.
- Tanwar, L., Börgel, J., and Ritter, T. (2019). Synthesis of benzylic alcohols by C–H oxidation. *J. Am. Chem. Soc.* 141, 17983–17988. <https://doi.org/10.1021/jacs.9b09496>.
- Tao, C., Wang, B., Sun, L., Liu, Z., Zhai, Y., Zhang, X., and Wang, J. (2017). Merging visible-light photoredox and copper catalysis in catalytic aerobic oxidation of amines to nitriles. *Org. Biomol. Chem.* 15, 328–332. <https://doi.org/10.1039/c6ob02510b>.
- Tao, X.-Z., Dai, J.-J., Zhou, J., Xu, J., and Xu, H.-J. (2018). Electrochemical C–O bond formation: facile access to aromatic lactones. *Chem. Eur. J.* 24, 6932–6935. <https://doi.org/10.1002/chem.201801108>.
- Trammell, R., Rajabimoghadam, K., and Garcia-Bosch, I. (2019). Copper-Promoted functionalization of organic molecules: from biologically relevant Cu/O₂ model systems to organometallic transformations. *Chem. Rev.* 119, 2954–3031. <https://doi.org/10.1021/acs.chemrev.8b00368>.

- Tran, B.L., Driess, M., and Hartwig, J.F. (2014). Copper-catalyzed oxidative dehydrogenative carboxylation of unactivated alkanes to allylic esters via alkenes. *J. Am. Chem. Soc.* *136*, 17292–17301. <https://doi.org/10.1021/ja510093x>.
- Van Velthoven, N., Wang, Y., Van Hees, H., Henrion, M., Bugaev, A.L., Gracy, G., Amro, K., Soldatov, A.V., Alauzun, J.G., Mutin, P.H., and De Vos, D.E. (2020). Heterogeneous single-site catalysts for C–H activation reactions: Pd(II)-Loaded S,O-functionalized metal oxide-bisphosphonates. *ACS Appl. Mater. Inter.* *12*, 47457–47466. <https://doi.org/10.1021/acscami.0c12325>.
- Vasilopoulos, A., Zultanski, S.L., and Stahl, S.S. (2017). Feedstocks to pharmacophores: Cu-catalyzed oxidative arylation of inexpensive alkylarenes enabling direct access to diarylalkanes. *J. Am. Chem. Soc.* *139*, 7705–7708. <https://doi.org/10.1021/jacs.7b03387>.
- Wang, X., Gallardo-Donaire, J., and Martin, R. (2014). Mild ArI-catalyzed C(sp²)-H or C(sp³)-H functionalization/C–O formation: an intriguing catalyst-controlled selectivity switch. *Angew. Chem. Int. Ed.* *53*, 11084–11087. <https://doi.org/10.1002/ange.201407011>.
- Wang, S.-F., Cao, X.-P., and Li, Y. (2017). Efficient aryl migration from an aryl ether to a carboxylic acid group to form an ester by visible-light photoredox catalysis. *Angew. Chem. Int. Ed.* *56*, 13809–13813. <https://doi.org/10.1002/ange.201706597>.
- Wang, C.-Y., Qin, Z.-Y., Huang, Y.-L., Jin, R.-X., Lan, Q., and Wang, X.-S. (2019). Enantioselective copper-catalyzed cyanation of remote C(sp³)-H bonds enabled by 1,5-hydrogen atom transfer. *iScience* *21*, 490–498. <https://doi.org/10.1016/j.isci.2019.10.048>.
- Wootton, R.C.R., Fortt, R., and de Mello, A.J. (2002). A microfabricated nanoreactor for safe, continuous generation and use of singlet oxygen. *Org. Proc. Res. Dev.* *6*, 187–189. <https://doi.org/10.1021/op0155155>.
- Wu, G., Guo, H.-F., Gao, K., Liu, Y.-N., Bastow, K.F., Morris-Natschke, S.L., Lee, K.-H., and Xie, L. (2008). Synthesis of unsymmetrical biphenyls as potent cytotoxic agents. *Bioorg. Med. Chem. Lett.* *18*, 5272–5276. <https://doi.org/10.1016/j.bmcl.2008.08.050>.
- Xia, Q., Liu, X., Zhang, Y., Chen, C., and Chen, W. (2013). Copper-catalyzed N-methylation of amides and O-methylation of carboxylic acids by using peroxides as the methylating reagents. *Org. Lett.* *15*, 3326–3329. <https://doi.org/10.1021/ol401362k>.
- Yang, Q., Jia, Z., Li, L., Zhang, L., and Luo, S. (2018). Visible-light promoted arene C–H/C–X lactonization via carboxylic radical aromatic substitution. *Org. Chem. Front.* *5*, 237–241. <https://doi.org/10.1039/c7qo00826k>.
- Yi, H., Zhang, G., Wang, H., Huang, Z., Wang, J., Singh, A.K., and Lei, A. (2017). Recent advances in radical C–H activation/radical cross-coupling. *Chem. Rev.* *117*, 9016–9085. <https://doi.org/10.1021/acs.chemrev.6b00620>.
- Zhang, X.-S., Zhang, Y.-F., Li, Z.-W., Luo, F.-X., and Shi, Z.-J. (2015). Synthesis of Dibenzo[*c,e*]oxepin-5(7H)-ones from Benzyl Thioethers and Carboxylic Acids: rhodium-Catalyzed Double C–H Activation Controlled by Different Directing Groups. *Angew. Chem. Int. Ed.* *54*, 5478–5482. <https://doi.org/10.1002/ange.201500486>.
- Zhang, M., Ruzi, R., Li, N., Xie, J., and Zhu, C. (2018a). Photoredox and cobalt Co-catalyzed C(sp²)-H functionalization/C–O bond formation for synthesis of lactones under oxidant- and acceptor-free conditions. *Org. Chem. Front.* *5*, 749–752. <https://doi.org/10.1039/c7qo00795g>.
- Zhang, S., Li, L., Wang, H., Li, Q., Liu, W., Xu, K., and Zeng, C. (2018b). Scalable electrochemical dehydrogenative lactonization of C(sp²/sp³)-H bonds. *Org. Lett.* *20*, 252–255. <https://doi.org/10.1021/acs.orglett.7b03617>.
- Zhang, G., Fu, L., Chen, P., Zou, J., and Liu, G. (2019). Proton-coupled electron transfer enables tandem radical relay for asymmetric copper-catalyzed phosphinoylcyanation of styrenes. *Org. Lett.* *21*, 5015–5020. <https://doi.org/10.1021/acs.orglett.9b01607>.
- Zheng, Y.-W., Narobe, R., Donabauer, K., Yakubov, S., and König, B. (2020). Copper(II)-Photocatalyzed N–H alkylation with alkanes. *ACS Catal.* *10*, 8582–8589. <https://doi.org/10.1021/acscatal.0c01924>.
- Zhuang, Z., and Yu, J.-Q. (2020). Lactonization as a general route to β-C(sp³)-H functionalization. *Nature* *577*, 656–659. <https://doi.org/10.1038/s41586-019-1859-y>.

STAR★METHODS

KEY RESOURCES TABLE

REAGENT or RESOURCE	SOURCE	IDENTIFIER
Chemicals, peptides, and recombinant proteins		
Copper (powder, <425 μm, 99.5% trace metals basis)	Sigma Aldrich	CAS 7440-50-8
2-iodobenzoic acid	Sigma Aldrich	CAS 88-67-5
4-iodo-2-methoxybenzoic acid	Sigma Aldrich	CAS 89942-34-7
5-chlorosalicylic acid	Sigma Aldrich	CAS 321-14-2
4-Nitrosalicylic Acid	TCI	CAS 619-19-2
4-Fluoro-2-iodobenzoic acid	Sigma Aldrich	CAS 56096-89-0
5-Fluoro-2-iodobenzoic Acid	TCI	CAS 52548-63-7
4-Methylsalicylic acid	Sigma Aldrich	CAS 50-85-1
3-Fluorosalicylic Acid	TCI	CAS 341-27-5
2-Hydroxy-1-naphthoic acid	Sigma Aldrich	CAS 2283-08-1
o-Tolylboronic acid	Sigma Aldrich	CAS 16419-60-6
2,6-Dimethylphenylboronic acid	Sigma Aldrich	CAS 100379-00-8
2,5-Dimethylphenylboronic acid	TCI	CAS 85199-06-0
4-Methoxy-2-methylbenzeneboronic acid	Acros	CAS 208399-66-0
(4-Bromo-2-methylphenyl)boronic acid	Sigma Aldrich	CAS 221006-71-9
2,4,6-Trimethylphenylboronic acid	Sigma Aldrich	CAS 5980-97-2
2-Ethylphenylboronic acid	TCI	CAS 90002-36-1
2,5-Dimethyl-4-methoxyphenylboronic acid	TCI	CAS 246023-54-1
4-Ethoxy-2-methylphenylboronic Acid	TCI	CAS 313545-31-2
4-Chloro-2-methylphenylboronic Acid	TCI	CAS 209919-30-2
K ₂ CO ₃	Spectrochem	CAS 584-08-7
Pd(PPh ₃) ₄	Sigma Aldrich	CAS 14221-01-3
Di-tert-butyl peroxide	Sigma Aldrich	CAS 110-05-4
Rose bengal	Sigma Aldrich	CAS 632-69-9
α,α,α-Trifluorotoluene	Sigma Aldrich	CAS 98-08-8
TEMPO	Sigma Aldrich	CAS 2564-83-2
Cu(OAc) ₂	Sigma Aldrich	CAS 142-71-2
Benzoyl peroxide	Sigma Aldrich	CAS 94-36-0
SPhos	Sigma Aldrich	CAS 657408-07-6
Lawesson's reagent	Sigma Aldrich	CAS 19172-47-5
Deposited data		
11-methyldibenzo[c,e]oxepin-5(7H)-one	CCDC	CCDC No. 2105616
7-phenyldibenzo[c,e]oxepin-5(7H)-one	CCDC	CCDC No. 2105617

RESOURCE AVAILABILITY

Lead contact

Further information and requests for resources should be directed to and will be fulfilled by the lead contact, Ranjan Jana (rjana@iicb.res.in).

Materials availability

All other data supporting the findings of this study are available within the article and the [supplemental information](#) or from the [lead contact](#) upon reasonable request.

Data and code availability

All original crystal structures have been deposited at CCDC and is publicly available as of the date of publication. CCDC numbers are listed in the key resources table. Any additional information required to re-analyze the data reported in this paper is available from the [lead contact](#) upon request.

METHOD DETAILS

General reagent information

All manipulations with air-sensitive reagents were carried out under a dry argon atmosphere. Unless otherwise stated, all commercial reagents were purchased from Sigma Aldrich, TCI, Acros or Spectrochem chemical companies and used without additional purification. Solvents were dried using standard methods and distilled before use. TLC was performed on silica gel plates (Merck silica gel 60, f254), and the spots were visualized with UV light (254 and 365 nm) or by charring the plate dipped in KMnO₄ or vanillin charring solution.

General analytical information

¹H NMR was recorded at 300 MHz (Bruker-DPX), 400 MHz (JEOL-JNMECZ400S/L1) and 600 MHz (Bruker-Avance) frequency and ¹³C NMR spectra were recorded at 75 MHz (Bruker-DPX) 100 MHz (JEOL-JNMECZ400S/L1) and 150 MHz (Bruker-Avance) frequency in CDCl₃ solvent using TMS as the internal standard. Chemical shifts were measured in parts per million (ppm) referenced to 0.0 ppm for tetramethylsilane. The following abbreviations were used to explain multiplicities: s = singlet, d = doublet, t = triplet, q = quartet, m = multiplet, br = broad, AB_q = AB quartet. Coupling constants, J were reported in Hertz unit (Hz). HRMS (*m/z*) were measured using ESI technique (Q-ToF Micro mass spectrometer). Crystals were grown in dichloromethane and crystal data was recorded in Bruker D8 Venture with a Photon-III detector instrument. Room temperature absorption spectra were recorded with a Shimadzu-made UV-vis spectrophotometer using a cuvette with a path length of 1 cm. The emission spectra of all of the samples were taken with a FluoroMax-P (HORIBA JobinYvon) luminescence spectrophotometer. The transmission electron microscopic (TEM) and scanning transmission electron microscopic (STEM) images were captured using a JEOL JEM 2100F transmission electron microscope. The X-ray photoelectron spectroscopy (XPS) measurements were performed with an Omicron electron spectrometer, equipped with a Scienta Omicron SPHERA analyzer. The gas evolved during reaction was detected by using GC instrument of model no. 7890B (G3440B), serial no. CN14333203 fitted with TCD. 500 μL gas was syringed out by a gas tight syringe from the head space of the working chamber of the H cell and was injected into the inlet of the GC.

General procedure for preparation of starting materials 2'-alkyl-[1,1'-biphenyl]-2-carboxylic acids (1)

This was performed following a method modified from literature procedure (Li et al., 2019).

General procedure for preparation of ethyl esters of 2-iodo/bromo benzoic acids or salicylic acids (Carrillo-Arcos et al., 2016)

Corresponding acid (5 mmol) was taken in oven dried RB and dissolved in 15 mL MeOH. To this solution 10 drops of concentrated H₂SO₄ was added and refluxed overnight at 80°C in oil bath. Then solvent was evaporated in rotary evaporator and the reaction mixture was transferred in a separating funnel with ethyl acetate and washed with water. The organic layer was dried over sodium sulfate and concentrated under vacuum. The resulting crude product was purified by column chromatography eluting pet ether/ethyl acetate (Scheme S1).

General procedure for preparation of methyl 2-(((trifluoromethyl)sulfonyl)oxy)benzoate from methyl salicylates

To a stirred solution of methyl salicylate (5mmol) in anhydrous DCM (10 mL) at 0°C was added triethylamine (1.4 mL, 2eq). Thereafter, trifluoromethanesulfonic anhydride (1 mL, 6 mmol) dropwise over 5 min at 0°C. The clear colourless solution was allowed to return slowly to room temperature. After 16 h the reaction was quenched with water, extracted with CH₂Cl₂ (5 × 15 mL) and the organic phase washed with water (20 mL) and brine (10 mL). The organic phase was dried over anhydrous sodium sulfate, filtered and the solvent removed in vacuo to give a liquid. After purification by column chromatography, eluting with ethyl acetate in hexanes, methyl 2-(((trifluoromethyl)sulfonyl)oxy)benzoate was obtained as a clear colourless liquid (Scheme S2).

General procedure for Suzuki coupling between 2-alkyl aryl boronic acid and 2-iodo/bromo benzoate or methyl 2-(((trifluoromethyl)sulfonyl)oxy)benzoate

To a solution of corresponding 2-iodo/bromo benzoate or methyl 2-(((trifluoromethyl)sulfonyl)oxy)benzoate (1 mmol) in dry DMF (5 mL) was added appropriate 2-alkyl aryl boronic acid (1.2 mmol, 1.2 equiv), activated K_2CO_3 (3mmol, 3 equiv) and $Pd(PPh_3)_4$ (5 mol%). The resulting solution was stirred at 90°C under argon atmosphere for 20 h. After completion of the reaction, the resulting reaction mixture was diluted with ethyl acetate and washed with ice-cold water (20 mL) followed by brine solution (20 mL) and dried over activated Na_2SO_4 , and evaporated in vacuo. The crude mixture was loaded on a silica gel column chromatography and purified using (Hexane/EtOAc) to give the desired ester product (Scheme S3).

General procedure for hydrolysis of methyl esters

Corresponding ester was dissolved in a NaOH solution of ethanol-water (1:1), and the reaction mixture was stirred at 60°C in oil bath for overnight. Then the reaction mixture was evaporated with rotary evaporator and the residue was neutralized with 6 (N) HCl. The solution was extracted with ethyl acetate and concentrated. Then purified the residue by column chromatography eluting pet ether/ethyl acetate and thus the final substrate 2'-alkyl-[1,1'-biphenyl]-2-carboxylic acid one is yielded (Scheme S4).

General experimental procedure for the preparation of 2-aryloxybenzoic acids (3)

These compounds were prepared from following literature procedure. To an oven-dried 100 mL round bottom flask equipped with magnetic stir bar, 2-halobenzoic acid (6.2 mmol, 1.0 equiv) was added in 50 mL of dimethylformamide (DMF), followed by corresponding phenol (12.4 mmol, 2.0 equiv), 1,8-diazabicyclo [5.4.0]undec-7-ene (DBU) (2.6 mL, 18.6 mmol, 3.0 equiv), pyridine (0.1 mL), copper(0) (52 mg, 0.81 mmol), and copper(I) iodide (53 mg, 0.28 mmol). The reaction mixture was heated to 160°C under nitrogen atmosphere. After consumption of the starting materials as indicated by TLC (typically 2 h) the reaction mixture was cooled and acidified with 3 M HCl until no more precipitate was formed. The resulting precipitates and reaction mixture were extracted with dichloromethane (60 mL) and cold water (70 mL). The organic layer was washed with cold water (20 mL \times 3) and brine (10 mL), dried over anhydrous Na_2SO_4 and the solvent was evaporated under reduced pressure. The crude product was purified by column chromatography using ethyl acetate-hexane as eluent to afford the desired white solid product.

Preparation of starting materials 2-alkyl-2'-methyl-1,1'-biphenyls (5)

To a solution of corresponding 2-iodo toluene (1 mmol) in toluene (4 mL) and ethanol (2 mL) was added appropriate 2-alkyl aryl boronic acid (1.2 mmol, 1.2 equiv), activated K_2CO_3 (3mmol, 3 equiv) and $Pd(PPh_3)_4$ (5 mol%). The resulting solution was stirred at 90°C under argon atmosphere for 20 h. After completion of the reaction, the resulting reaction mixture was diluted with ethyl acetate and washed with water (20 mL) followed by brine solution (20 mL) and dried over activated Na_2SO_4 , and evaporated in vacuo. The crude mixture was loaded on a silica gel column chromatography and purified using (Hexane/EtOAc) to give the desired 2-alkyl-2'-methyl-1,1'-biphenyl 5.

Reaction profile of the standard reaction under condition A and B (Scheme 2)

General condition A

A mixture of substrate 1 (0.2 mmol), copper powder (2.54 mg, 0.04 mmol, 20 mol %) was taken in a 15-mL pressure tube. To this reaction mixture, $PhCF_3$ solvent (2 mL) was added via syringe. To this, DTBP (36.7 μ L, 0.4 mmol, 2 equiv) was added and the vessel was closed. The reaction mixture was allowed to stir at 110°C for 36 h. After completion as indicated by TLC, the reaction mixture was cooled to ambient temperature and quenched with water (30 mL). The reaction mixture was extracted with ethyl acetate (2 \times 30 mL) in a separatory funnel. The combined organic layers were washed with brine, dried over anhydrous Na_2SO_4 , and concentrated under reduced pressure. The crude product was purified by column chromatography using ethyl acetate/hexane as eluent to afford the corresponding dibenzooxepinones derivatives.

General condition B

A mixture of substrate 1 (0.2 mmol), copper powder (0.04 mmol, 20 mol %) and rose bengal (RB, 0.002 mmol, 1 mol%) was taken in a 15-mL pressure tube. To this reaction mixture, $PhCF_3$ solvent (2 mL) was added via micro pipette. The vessel was purged with O_2 and closed. The reaction mixture was allowed to stir at 110°C under irradiation from two white CFL lamps (32 W, each 5cm apart from reaction vessel) for 30h. After completion as indicated by TLC, the reaction mixture was cooled to ambient temperature and

quenched with water (30 mL). The reaction mixture was extracted with ethyl acetate (2x30 mL) in a separatory funnel. The combined organic layers were washed with brine, dried over anhydrous Na₂SO₄, and concentrated under reduced pressure. The crude product was purified by column chromatography using ethyl acetate/hexane as eluent to afford the corresponding dibenzooxepinones derivatives.

General experimental procedure for the carboxyl radical assisted 1,5-aryl migration through Smiles rearrangement using 2-phenoxybenzoic acids, Scheme 4

To an oven-dried 15 mL sealed tube, 2-phenoxybenzoic acids (0.2 mmol, 1.0 equiv), copper(0) powder were taken and dry PhCF₃ (2.0 mL) was added to it. Subsequently DTBP (0.4 mmol, 2 equiv) was added. The vessel was sealed with a screw cap and the reaction mixture was allowed to stir for 36 h at 110°C. After completion (as indicated by TLC), the reaction mixture was cooled to room temperature. Then the reaction mixture was poured into water (20 mL) and extracted with ethyl acetate (20 mL). The organic layer was washed with water (10 mL) and brine (10 mL), dried over anhydrous Na₂SO₄ and the solvent was evaporated under reduced pressure. The crude product was purified by column chromatography using ethyl acetate-hexane as eluent to afford the desired product.

General experimental procedures for copper-catalyzed chemo- and regioselective double C-H activation of 2-alkyl-2'-methyl-1,1'-biphenyls (5), Scheme 5

A mixture of substrate **5** (0.2 mmol), copper powder (0.04 mmol, 20 mol %) was taken in a 15-mL pressure tube. To this reaction mixture, PhCF₃ solvent (2 mL) was added via micro pipette. To this, DTBP (0.4 mmol, 2 equiv) was added. UHP oxygen was purged and subsequently the vessel was closed. The reaction mixture was allowed to stir at 110°C for 36 h. After completion as indicated by TLC, the reaction mixture was cooled to ambient temperature and quenched with water (30 mL). The reaction mixture was extracted with ethyl acetate (2x30 mL) in a separating funnel. The combined organic layer was washed with brine, dried over anhydrous Na₂SO₄, and concentrated under reduced pressure. The crude product was purified by column chromatography using ethyl acetate/hexane as eluent to afford the corresponding dibenzooxepinones derivatives.

Experimental procedure for total synthesis of alterlactone (21)

Please see Scheme S5 for the synthesis.

5,7-Dihydroxy-2,2-dimethyl-4H-benzo[d][1,3]dioxin-4-one (7)

This was prepared according to modified method from previously reported literature. To an ice-cold solution of 2,4,6-trihydroxybenzoic acid monohydrate **6** (10.0 g, 58.8 mmol) in trifluoroacetic acid (100 mL), were added trifluoroacetic anhydride (70 mL) and acetone (15 mL). The mixture was warmed slowly to room temperature and stirred for 12 h. The reaction mixture was concentrated under reduced pressure, poured into a saturated aqueous NaHCO₃ solution (200 mL) and extracted with ethyl acetate (3 × 200 mL). The combined extracts were washed with water (2 × 300 mL), brine (2 × 300 mL), dried over Na₂SO₄ and concentrated under reduced pressure. The crude product was purified by column chromatography over silica gel (ethyl acetate/hexane = 1:4) to afford **7** (9.7 g, 79%) as light-yellow solid. R_f 0.52 (4:1 hexane/ethyl acetate).

5-Hydroxy-7-methoxy-2,2-dimethyl-4H-benzo[d][1,3]dioxin-4-one (8)

To a stirred solution of compound **7** (4.5 g, 21.4 mmol) and methanol (0.9 mL, 23.5 mmol) in CH₂Cl₂ (45 mL) at 0°C, were added triphenyl phosphine (6.2 g, 23.5 mmol) and DIAD (4.6 mL, 23.5 mmol). The reaction mixture was warmed to room temperature and stirred for 3 h. After completion of the reaction (monitored by TLC), it was quenched with water (30 mL). The organic layer was separated and the aqueous layer was extracted with CH₂Cl₂ (2 × 50 mL). The combined organic layers were washed with water (70 mL), brine (70 mL), dried over anhydrous Na₂SO₄ and concentrated under reduced pressure. The crude mass was purified by silica gel column chromatography (ethyl acetate/hexane = 1:10) to furnish compound **8** (4.6 g, 95%) as white solid. R_f 0.55 (4:1 hexane/ethyl acetate).

7-Methoxy-2,2-dimethyl-4-oxo-4H-benzo[d][1,3]dioxin-5-yl trifluoromethanesulfonate (9)

Anhydrous pyridine (4.2 mL, 51.5 mmol) and trifluoromethanesulfonic anhydride (6.5 mL, 38.6 mmol) were successively added to a solution of 5-hydroxy-2,2-dimethyl-4H-benzo[d][1,3]dioxin-4-one (**8**) (5.0 g, 25.7 mmol) in anhydrous dichloromethane (50 mL) and the mixture was allowed to stirred at 0°C for 2 h.

The reaction was quenched with water (50 mL) and the reaction mixture was extracted with dichloromethane (3 × 50 mL). The combined organic layer was dried over anhydrous Na₂SO₄ and concentrated under reduced pressure. The crude product was purified by silica gel column chromatography (ethyl acetate/hexane = 1:3) to afford **9** (7.7 g, 92%) as a colorless solid. R_f 0.57 (9:1 hexane/ethyl acetate).

4-Bromo-5-methylbenzene-1,2-diol (**11**)

This was prepared according to a reported procedure.⁶ To a 0°C solution of 4-methylcatechol (**10**) (1.24 g, 10 mmol, 1 equiv) in 10 mL acetonitrile was added a solution of NBS (1.86 g, 10.5 mmol, 1.05 equiv) in 10 mL MeCN. The solution was allowed to reach room temperature and stirred for additional 20 min. The reaction was quenched with water (100 mL) and washed with EtOAc (3 × 50 mL). The combined organic layer was dried over anhydrous Na₂SO₄ and concentrated under reduced pressure to yield 4-bromo-5-methylbenzene-1,2-diol (**11**) (2 g, 99%) as a white solid. This was used for the next step without further purification.

(((4-Bromo-5-methyl-1,2-phenylene)bis(oxy))bis(methylene))dibenzene (**12**)

This was prepared by benzylation of **11** by trival benzylation procedure of phenol. In a 100 mL round bottom flask closed with guard tube, suspension of compound **11** (1 g, 5 mmol, 1 equiv) and K₂CO₃ (1.7 g, 12.5 mmol, 2.5 equiv) in DMF solvent (20 mL) was stirred for 15 min at room temperature. Then BnBr (1.5 mL, 12.5 mmol, 2.5 equiv) was added dropwise and again the flask was closed with guard tube and allowed to stir at room temperature for additional 5 h. Thereafter, the reaction was quenched with ice-cold water (50 mL) and washed with ethyl acetate (3 × 50 mL). The combined organic layer was dried over anhydrous Na₂SO₄ and concentrated under reduced pressure. The crude product was purified by silica gel column chromatography (ethyl acetate/hexane = 5:95) to yield (((4-bromo-5-methyl-1,2-phenylene)bis(oxy))bis(methylene))dibenzene (**12**) (1.81 g, 95%) as a colourless gel.

2-(4,5-bis(benzyloxy)-2-methylphenyl)-4,4,5,5-tetramethyl-1,3,2-dioxaborolane (**13**)

To a solution of bromo arene **12** (1.15 g, 3 mmol, 1 equiv) and bis(pinacolato)diboron (839 mg, 1.1 equiv) in dioxane (15 mL) taking in a 30 mL pressure tube was added PdCl₂ (26.6 mg, 5 mol%), DPPF (166.3 mg, 10 mol%), potassium acetate (590 mg, 2 equiv). The reaction vessel was closed under argon atmosphere and was stirred for 20 h at 110°C. Then the reaction medium was diluted with water (50 mL) and washed with ethyl acetate (3 × 50 mL). The combined organic layer was dried over anhydrous Na₂SO₄ and concentrated under reduced pressure. The crude product was purified by silica gel column chromatography (ethyl acetate/hexane = 1:9) to yield the borylated compound **13** (1.16 g, 90%) as white solid.

5-(4,5-bis(benzyloxy)-2-methylphenyl)-7-methoxy-2,2-dimethyl-4H-benzo[d][1,3]dioxin-4-one (**14**)

Aryl triflate **9** (356 mg, 1.00 mmol), boronate **13** (516 mg, 1.20 mmol), Cs₂CO₃ (813 mg, 2.50 mmol), PdCl₂ (8.8 mg, 5 mol%) and S-Phos (purity 97%, 41.0 mg, 10 mol%) were dissolved under an Ar atmosphere in degassed dioxane/H₂O (7:1, 10 mL) and the mixture was stirred for 20 h at 80°C (monitoring with TLC) and cooled. Saturated NH₄Cl solution (10 mL) was added and the mixture was extracted with EtOAc (2 × 25 mL). The organic layers were dried over Na₂SO₄ and concentrated and the residue was purified by chromatography (silica gel, cyclohexane/EtOAc, 10:1) to yield coupling product **14** (428.4 mg, 84%) as colourless gel.

Benzyl 3,4',5'-tris(benzyloxy)-5-methoxy-2'-methyl-[1,1'-biphenyl]-2-carboxylate (**15**)

This was prepared by a modified method from literature report (Carrillo-Arcos et al., 2016). To a solution of **14** (325 mg, 0.5 mmol, 1 equiv) in DMF-water (5 mL, 8:1) taking in a 25 mL round bottom flask with guard tube was added NaH (60% purity, 30 mg, 1.5 equiv) at 0°C and stirred for 10 min. Then BnBr (1.48 mL, 2.5 equiv) was added dropwise at 0°C with continuous stirring. The reaction mixture was allowed to reach room temperature and stirred for 20 h. After completion of reaction acc. TLC, ice-cold water (10 mL) was added and washed with ethyl acetate (2 × 25 mL). The combined organic layer was dried over activated sodium sulfate and evaporated under reduced pressure to afford the crude product **15**. This was used for next step without further purification.

3,4',5'-tris(benzyloxy)-5-methoxy-2'-methyl-[1,1'-biphenyl]-2-carboxylic acid (**16**)

Corresponding crude ester **15** was dissolved in a KOH (168 mg, 6 equiv) solution of ethanol-water (1:1), and the reaction mixture was refluxed at 100°C with continuous stirring for 24 h. Then the reaction mixture was evaporated under reduced pressure and the residue was neutralized with 6 (N) HCl. The solution was

extracted with ethyl acetate and concentrated. Then purified the residue by column chromatography eluting pet ether/ethyl acetate (7:3) and thus the actual acid precursor **16** (243 mg, 87%) is yielded as white solid.

4,9,10-tris(benzyloxy)-2-methoxydibenzo[c,e]oxepin-5(7H)-one (17)

A mixture of substrate **16** (56 mg, 0.1 mmol), copper powder (1.2 mg, 0.04 mmol, 20 mol %) and rose bengal (RB, 1 mg, 0.002 mmol, 1 mol%) was taken in a 15-mL pressure tube. To this mixture, PhCF₃ solvent (2 mL) was added via micro pipette. The vessel was purged with O₂ and closed. The reaction mixture was allowed to stir at 110°C under irradiation from two white CFL lamps (32 W, each 5 cm apart from reaction vessel) for 30h. After completion as indicated by TLC, the reaction mixture was cooled to ambient temperature and quenched with water (30 mL). The reaction mixture was extracted with ethyl acetate (2x30 mL) in a separatory funnel. The combined organic layers were washed with brine, dried over anhydrous Na₂SO₄, and concentrated under reduced pressure. The crude mixture was purified by column chromatography using ethyl acetate/hexane (1:9) as eluent to afford the corresponding protected Alterlactone **17** (42.8 mg, 77%) as colourless gel.

4,9,10-Trihydroxy-2-methoxydibenzo[c,e]oxepin-5(7H)-one, alterlactone (18)

Pd/C (10%, 32.0 mg, 300 μmol) was added to a solution of protected alterlactone **17** (27.9 mg, 50.0 μmol) in EtOAc (0.05 mL) and EtOH (0.5 mL). The atmosphere was replaced with H₂ and the mixture was stirred for 7 h at rt (monitoring with TLC). The mixture was filtered and the filtrate was concentrated to yield alterlactone (**18**) as a colourless solid (14 mg, 50.0 μmol, quant.).

Derivatization procedures

Thiolation of dibenzo[c,e]oxepin-5(7H)-one (2a) to synthesize Dibenzo[c,e]oxepan-5-thione (DOT, 19)

Lactone dibenzo[c,e]oxepan-5-one **2a** (42 mg, 0.2 mmol) was dissolved in anhydrous toluene (2 mL) before an addition of Lawesson's Reagent (57 mg, 0.12 mmol, 0.6 equiv) and was refluxed for 22 h. Upon completion the reaction mixture was concentrated in vacuo and purified by column chromatography (Hex–EtOAc, 4:1) to afford yellow crystals (19.43 mg, 43%) (Scheme S6) (Bingham and Roth, 2019).

Synthesis of 2'-(hydroxymethyl)-[1,1'-biphenyl]-2-carboxylic acid (20)

Dibenzo[c,e]oxepan-5-one **2a** (42 mg, 0.2 mmol) was dissolved in a KOH solution of ethanol-water (1:1), and the reaction mixture was refluxed in oil bath for overnight. Then the reaction mixture was evaporated with rotary evaporator and the residue was neutralized with 6 (N) HCl. The solution was extracted with ethyl acetate and concentrated. Then purified the residue by column chromatography eluting pet ether/ethyl acetate and thus the 2'-(hydroxymethyl)-[1,1'-biphenyl]-2-carboxylic acid (**20**) is yielded as white solid (42 mg, 92%) (Scheme S7).

Practical demonstrations

Intramolecular benzylic C-H oxidation of 2'-methyl-[1,1'-biphenyl]-2-carboxylic acid in copper bottle without any external catalyst

Substrate **1a** (424 mg, 2.0 mmol) was taken in a 500 mL washed and dried commercially available copper bottle. To this, PhCF₃ solvent (10 mL) was added via micro pipette. To this, DTBP (4.0 mmol, 2 equiv) was added and the bottle was closed. (N.B.: No external copper catalyst was added!) The reaction mixture was allowed to stir at 110°C for 36 h. After completion as indicated by TLC, the reaction mixture was cooled to ambient temperature and quenched with water (100 mL). The reaction mixture was extracted with ethyl acetate (2x100 mL) in a separating funnel. The combined organic layers were washed with brine, dried over anhydrous Na₂SO₄, and concentrated under reduced pressure. The crude product was purified by column chromatography using ethyl acetate/hexane as eluent to afford the corresponding dibenzo[c,e]oxepin-5(7H)-one **2a** (231 mg, 55%) as white solid (Scheme S8).

Copper-catalyzed chemo- and regioselective intramolecular benzylic C-H oxidation of 2'-methyl-[1,1'-biphenyl]-2-carboxylic acid 1a in gram-scale

A mixture of substrate **1a** (2.12 g, 10 mmol, 1 equiv), copper powder (127 mg, 2 mmol, 20 mol %) and rose bengal (RB, 98mg, 0.1 mmol, 1 mol%) was taken in a 100 mL pressure tube. To this reaction mixture, PhCF₃

solvent (20 mL) was added via micro pipette. The vessel was purged with O₂ and closed. The reaction mixture was allowed to stir at 110°C under irradiation from two white CFL lamps (32 W, each 5cm apart from reaction vessel) for 30h. After completion as indicated by TLC, the reaction mixture was cooled to ambient temperature and quenched with water (300 mL). The reaction mixture was extracted with ethyl acetate (2x300 mL) in a separating funnel. The combined organic layers were washed with brine, dried over anhydrous Na₂SO₄, and concentrated under reduced pressure. The crude product was purified by column chromatography using ethyl acetate/hexane (97:3) as eluent to afford the corresponding dibenzo[*c,e*]oxepin-5(7H)-one **2a** (1.42 g, 68%) as white solid (Scheme S9).

Synthesis of 2,6-dimethyl-3'-H-spiro[cyclohexane-1,1'-isobenzofuran]-2,5-diene-3',4-dione (24)

4'-hydroxy-2',6'-dimethyl-[1,1'-biphenyl]-2-carboxylic acid (**1ab**) was subjected to reaction condition A and B each in 0.2 mmol scale. And instead of the 8-membered lactone, under both the conditions, 2,6-dimethyl-3'-H-spiro[cyclohexane-1,1'-isobenzofuran]-2,5-diene-3',4-dione **24** was achieved (45.6 mg, 95% under condition A and 38.4 mg, 80% under condition B)(Li et al., 2019) .

Synthesis of 6a-methyl-5H-benzo[4,5][1,3]oxazino[3,2-*a*]indole-5,7(6aH)-dione (25)

Taking N-protected indole **1af** as substrate (0.2 mmol), we subjected condition A and B. Instead of getting the expected reaction, dearomatized stable lactone 25 in excellent yield by using condition A was achieved where condition B remained unfruitful. 6a-methyl-5H-benzo[4,5][1,3]oxazino[3,2-*a*]indole-5,7(6aH)-dione was furnished as green solid in good yield (46.6 mg, 88%).

Synthesis of 4-methyl-9H-fluoren-9-one (27)

When benzyl alcohol substrate **26** was taken (0.02 mmol) instead of benzoic acid, oxidation led to formation of fluorenone **27** in lieu the seven membered lactone in both the conditions (23.9 mg, 61% under condition A, and 11mg, 28% under condition B) as yellow solid (Fukuyama et al., 2014).

Synthesis of 6-(phenylsulfonyl)-6,7-dihydro-5H-dibenzo[*c,e*]azepin-5-one (29)

N-(2'-methyl-[1,1'-biphenyl]-2-yl)benzenesulfonamide **28** was prepared by coupling of **2a** with benzenesulfonamide. **28** was then subjected to our reaction conditions (0.1mmol scale) to check the possibility of eight membered lactam formation via C(sp³-H) activation. Delightfully, it gave rise to formation of expected 7-membered lactam compound **29** albeit lower yield under condition A (8.7 mg, 25%). Though, condition B was not fruitful here. Further improvements are being undergone by our group.

Synthesis of (E)-3-styrylisobenzofuran-1(3H)-one (31)

Starting material **30** was prepared from the heck reaction between methyl 2-iodobenzoate and allylbenzene. The double bond is delocalised over two styrenyl position. With the ambition of synthesizing eight membered lactone as shown in the scheme, we subjected **30** in our reaction conditions (0.02 mmol). Instead of the expected reaction, under condition A, 5-membered lactone forms to synthesize isobenzofuranone **32** (37.28 mg, 79%). (Krätzschar et al., 2015) The scopes and improvements of this transformation is being carried out at our laboratory.

Spectroscopic details

dibenzo[*c,e*]oxepin-5(7H)-one (2a, Scheme 2)

The same general procedures **A** and **B** both were followed. Column chromatography (SiO₂, eluting with 97:3 hexane/ethyl acetate) afforded the desired product as a white solid, (34.4 mg, 82% acc. to condition **A** and 30.2 mg, 72% acc. to condition **B**). mp 98–102°C. ¹H NMR (600 MHz, CDCl₃): δ 7.99 (d, *J* = 7.8 Hz, 1H), 7.65–7.69 (m, 2H), 7.61 (d, *J* = 7.8 Hz, 1H), 7.51–7.56 (m, 2H), 7.42–7.47 (m, 2H), 5.03 (d(br), *J* = 41.4 Hz, 2H); ¹³C NMR (150 MHz, CDCl₃): δ 170.23, 138.96, 137.25, 134.81, 132.55, 131.93, 130.65, 130.12, 128.67, 128.65, 128.55, 128.42, 69.18. HRMS (ESI, *m/z*) calcd. for C₁₄H₁₀O₂Na [M + Na]⁺: 233.0578; found: 233.0576.

11-methyldibenzo[*c,e*]oxepin-5(7H)-one (2b, Scheme 2)

The same general procedures **A** and **B** both were followed. Column chromatography (SiO₂, eluting with 97:3 hexane/ethyl acetate) afforded the desired product as a white solid, (35.4 mg, 79% acc. to condition **A** and 31.4 mg, 70% acc. to condition **B**). mp 110–112°C. ¹H NMR (600 MHz, CDCl₃): δ 7.89 (dd, *J*₁ = 7.8 Hz, *J*₂ = 1.2 Hz, 1H), 7.58 (td, *J*₁ = 7.8 Hz, *J*₂ = 1.2 Hz, 1H), 7.48 (dd, *J*₁ = 7.2 Hz, *J*₂ = 1.2 Hz, 1H), 7.38 (dd, *J*₁ =

6.6 Hz, $J_2 = 2.4$ Hz, 1H), 7.27–7.30 (m, 2H), 4.90 (AB_q, $J = 8$ Hz, 2H); ¹³C NMR (150 MHz, CDCl₃): δ 170.59, 137.54, 136.62, 135.97, 135.78, 132.87, 131.59, 130.83, 130.76, 130.30, 128.11, 126.23, 70.05, 21.28. HRMS (ESI, m/z) calcd. for C₁₅H₁₃O₂ [M + H]⁺: 225.1006; found: 225.1205.

3-Methoxy-11-methyldibenzo[*c,e*]oxepin-5(7H)-one (2c, Scheme 2)

The same general procedures **A** and **B** both were followed. Column chromatography (SiO₂, eluting with 19:1 hexane/ethyl acetate) afforded the desired product as a white solid, (34.0 mg, 67% acc. to condition **A** and 27.0 mg, 53% acc. to condition **B**). mp 118–120°C. ¹H NMR (400 MHz, CDCl₃): δ 7.34–7.40 (m, 3H), 7.24–7.26 (m, 2H), 7.12 (dd, $J_1 = 8$ Hz, $J_2 = 4$ Hz, 1H), 4.90 (AB_q, $J = 12$ Hz, 2H), 3.89 (s, 3H); ¹³C NMR (100 MHz, CDCl₃): δ 170.54, 159.09, 137.52, 136.53, 135.81, 132.91, 132.81, 131.86, 128.49, 127.69, 126.25, 118.21, 114.30, 70.31, 55.70, 21.40. HRMS (ESI, m/z) calcd. for C₁₆H₁₄O₃Na [M + Na]⁺: 277.0841; found: 277.0841.

3-methoxydibenzo[*c,e*]oxepin-5(7H)-one (2d, Scheme 2)

The same general procedures **A** and **B** both were followed. Column chromatography (SiO₂, eluting with 19:1 hexane/ethyl acetate) afforded the desired product as a white solid, (29.4 mg, 61% acc. to condition **A** and 26.2 mg, 54% acc. to condition **B**). mp 116–122°C. ¹H NMR (600 MHz, CDCl₃): δ 7.61 (d, $J = 7.8$ Hz, 1H), 7.51–7.55 (m, 2H), 7.48 (d, $J = 3$ Hz, 1H), 7.45 (dd, $J_1 = 7.2$ Hz, $J_2 = 1.2$ Hz, 1H), 7.39 (td, $J_1 = 7.2$ Hz, $J_2 = 1.2$ Hz, 1H), 7.22 (dd, $J_1 = 9$ Hz, $J_2 = 3$ Hz, 1H), 5.01 (d(br), $J = 30.6$ Hz, 2H), 3.91 (s, 3H); ¹³C NMR (150 MHz, CDCl₃): δ 170.06, 159.46, 138.77, 134.32, 131.69, 131.60, 130.16, 130.04, 128.44, 128.16, 127.96, 120.04, 115.20, 69.34, 55.64. HRMS (ESI, m/z) calcd. for C₁₅H₁₂O₃Na [M + Na]⁺: 263.0684; found: 263.0690.

10-methyldibenzo[*c,e*]oxepin-5(7H)-one (2e, Scheme 2)

The same general procedures **A** and **B** both were followed. Column chromatography (SiO₂, eluting with 97:3 hexane/ethyl acetate) afforded the desired product as a gummy syrup, (25.8 mg, 58% acc. to condition **A** and 27.2 mg, 61% acc. to condition **B**). ¹H NMR (600 MHz, CDCl₃): δ 7.96 (dd, $J_1 = 7.8$ Hz, $J_2 = 1.2$ Hz, 1H), 7.64 (td, $J_1 = 7.8$ Hz, $J_2 = 1.2$ Hz, 1H), 7.58–7.59 (m, 1H), 7.49 (td, $J_1 = 7.2$ Hz, $J_2 = 1.2$ Hz, 1H), 7.44 (s, 1H), 7.33 (d, $J = 7.8$ Hz, 1H), 7.22 (d, $J = 7.8$ Hz, 1H), 5.04 (AB_q, $J = 12$ Hz, 2H), 2.43 (s, 3H); ¹³C NMR (150 MHz, CDCl₃): δ 170.36, 140.07, 138.86, 137.39, 132.43, 132.06, 131.89, 130.76, 129.28, 128.55, 128.47, 128.27, 68.93, 21.42. HRMS (ESI, m/z) calcd. for C₁₅H₁₃O₂ [M + H]⁺: 225.0916; found: 225.0919.

9-methoxydibenzo[*c,e*]oxepin-5(7H)-one (2f, Scheme 2)

The same general procedures **A** and **B** both were followed. Column chromatography (SiO₂, eluting with 19:1 hexane/ethyl acetate) afforded the desired product as a white solid, (38.0 mg, 79% acc. to condition **A** and 31.2 mg, 65% acc. to condition **B**). mp 155–158°C. ¹H NMR (400 MHz, CDCl₃): δ 7.95 (dd, $J_1 = 6$ Hz, $J_2 = 1.6$ Hz, 1H), 7.62 (td, $J_1 = 7.6$ Hz, $J_2 = 1.6$ Hz, 1H), 7.52–7.57 (m, 1H), 7.45 (td, $J_1 = 7.6$ Hz, $J_2 = 1.6$ Hz, 1H), 7.05 (dd, $J_1 = 8$ Hz, $J_2 = 1.6$ Hz, 1H), 6.97 (d, $J = 2.4$ Hz, 1H), 4.97 (d(br), $J = 40$ Hz, 2H), 3.87 (s, 3H); ¹³C NMR (100 MHz, CDCl₃): δ 170.48, 159.97, 137.35, 136.24, 132.62, 132.13, 131.51, 130.25, 10.02, 128.43, 127.85, 115.70, 113.94, 69.37, 55.62. HRMS (ESI, m/z) calcd. for C₁₅H₁₃O₂ [M + H]⁺: 241.0865; found: 241.0870.

9-Bromo-3-methoxydibenzo[*c,e*]oxepin-5(7H)-one (2g, Scheme 2)

The same general procedures **A** and **B** both were followed. Column chromatography (SiO₂, eluting with 19:1 hexane/ethyl acetate) afforded the desired product as a white solid, (42.6 mg, 67% acc. to condition **A** and 45.2 mg, 71% acc. to condition **B**). mp 172–178°C. ¹H NMR (400 MHz, CDCl₃): δ 8.09 (d, $J = 2.4$ Hz, 1H), 7.73 (dd, $J_1 = 8.4$ Hz, $J_2 = 2$ Hz, 1H), 7.53 (d, $J = 8.4$ Hz, 1H), 7.41 (d, $J = 8.4$ Hz, 1H), 7.05 (dd, $J_1 = 8.4$ Hz, $J_2 = 1.2$ Hz, 1H), 6.97 (d, $J = 1.4$ Hz, 1H), 4.97 (d(br), $J = 16.8$ Hz, 2H), 3.87 (s, 3H); ¹³C NMR (100 MHz, CDCl₃): δ 168.95, 160.25, 136.20, 136.00, 135.65, 134.72, 131.74, 130.43, 130.00, 129.89, 121.77, 115.87, 114.16, 69.40, 55.66. HRMS (ESI, m/z) calcd. for C₁₅H₁₂O₃Br [M + H]⁺: 318.9970; found: 318.9978.

2-chlorodibenzo[*c,e*]oxepin-5(7H)-one (2h, Scheme 2)

The same general procedures **A** and **B** both were followed. Column chromatography (SiO₂, eluting with 97:3 hexane/ethyl acetate) afforded the desired product as a white solid, (33.2 mg, 68% acc. to condition **A** and 34.2 mg, 70% acc. to condition **B**). mp 140–142°C. ¹H NMR (400 MHz, CDCl₃): δ 7.92 (d, $J = 12$ Hz, 1H), 7.63 (d, $J = 12$ Hz, 1H), 7.60 (d, $J = 4$ Hz, 1H), 7.53–7.57 (m, 1H), 7.45–7.49 (m, 3H), 5.01 (d(br), $J = 16$ Hz, 2H); ¹³C NMR (100 MHz, CDCl₃): δ 167.79, 139.00, 138.98, 137.85, 134.90, 133.68, 129.40, 129.12, 128.72, 128.69, 128.64, 69.22. HRMS (ESI, m/z) calcd. for C₁₄H₁₀O₂Cl [M + H]⁺: 245.0369; found: 245.0371.

11-Methyl-3-nitrodibenzo[*c,e*]oxepin-5(7*H*)-one (2i, Scheme 2)

The same general procedures A and B both were followed. Column chromatography (SiO₂, eluting with 97:3 hexane/ethyl acetate) afforded the desired product as a white solid, (30.1 mg, 57% acc. to condition A and 25.8 mg, 48% acc. to condition B). mp 198–200°C. ¹H NMR (400 MHz, CDCl₃): δ 8.76 (d, *J* = 2.4 Hz, 1H), 8.41 (dd, *J*₁ = 4.8 Hz, *J*₂ = 2.4 Hz, 1H), 7.67 (d, *J* = 4.8 Hz, 1H), 7.32–7.45 (m, 3H), 4.95 (ABq, *J* = 12.4 Hz, 2H), 2.43 (s, 3H); ¹³C NMR (100 MHz, CDCl₃): δ 168.26, 142.00, 137.08, 135.91, 133.50, 133.16, 131.79, 129.73, 126.87, 126.32, 125.22, 70.13, 21.30. HRMS (ESI, *m/z*) calcd. for C₁₅H₁₂NO₄ [M + H]⁺: 270.0766; found: 270.0769.

3-fluorodibenzo[*c,e*]oxepin-5(7*H*)-one (2j, Scheme 2)

The same general procedures A and B both were followed. Column chromatography (SiO₂, eluting with 19:1 hexane/ethyl acetate) afforded the desired product as a white solid, (31.0 mg, 68% acc. to condition A and 26.4 mg, 58% acc. to condition B). mp 166–168°C. ¹H NMR (400 MHz, CDCl₃): δ 7.69 (dd, *J*₁ = 9 Hz, *J*₂ = 3 Hz, 1H), 7.61–7.65 (m, 2H), 7.53 (td, *J*₁ = 7.8 Hz, *J*₂ = 1.8 Hz, 1H), 7.34–7.47 (m, 3H), 5.01 (d(br), *J* = 12 Hz, 2H); ¹³C NMR (100 MHz, CDCl₃): δ 168.93, 162.30 (d, *J*_{C-F} = 248.9 Hz), 138.13, 134.56, 133.65 (d, *J*_{C-F} = 3.5 Hz), 132.56, 132.49, 130.92 (d, *J*_{C-F} = 7.7 Hz), 130.37, 128.80 (d, *J*_{C-F} = 4 Hz), 128.57, 120.14 (d, *J*_{C-F} = 21.3 Hz), 118.61 (d, *J*_{C-F} = 23.6 Hz), 69.41. HRMS (ESI, *m/z*) calcd. for C₁₄H₁₀FO₂ [M + H]⁺: 229.0665; found: 229.0669.

2-Fluoro-9,11-dimethyldibenzo[*c,e*]oxepin-5(7*H*)-one (2k, Scheme 2)

The same general procedures A and B both were followed. Column chromatography (SiO₂, eluting with 19:1 hexane/ethyl acetate) afforded the desired product as a white solid, (36.8 mg, 72% acc. to condition A and 32.4 mg, 63% acc. to condition B). mp 174–176°C. ¹H NMR (600 MHz, CDCl₃): δ 7.89–7.91 (m, 1H), 7.20 (s, 1H), 7.13–7.17 (m, 2H), 7.10 (s, 1H), 4.87 (ABq, *J* = 36 Hz, 2H), 2.38 (s, 3H), 2.37 (s, 3H); ¹³C NMR (150 MHz, CDCl₃): δ 169.72, 163.52 (d, *J*_{C-F} = 251.2 Hz), 138.72, 138.70, 136.43, 135.80, 133.69, 133.47 (d, *J*_{C-F} = 9.3 Hz), 127.82, 127.13, 117.05 (d, *J*_{C-F} = 22.3 Hz), 115.1 (d, *J*_{C-F} = 21.4 Hz), 70.03, 21.09, 20.94. HRMS (ESI, *m/z*) calcd. for C₁₆H₁₃FO₂Na [M + Na]⁺: 279.0797; found: 279.0800.

2-Fluoro-7-methyldibenzo[*c,e*]oxepin-5(7*H*)-one (2L, Scheme 2)

The same general procedures A with additional amount of 2.0 equiv TEMPO and B both were followed. Column chromatography (SiO₂, eluting with 97:3 hexane/ethyl acetate) afforded the desired product as a gummy liquid, (25.6 mg, 53% acc. to condition A and 23.2 mg, 48% acc. to condition B). ¹H NMR (600 MHz, CDCl₃): δ 8.01–8.03 (m, 1H), 7.50–7.59 (m, 4H), 7.29 (dd, *J*₁ = 3.6 Hz, *J*₂ = 2.4 Hz, 1H), 7.51–7.56 (m, 2H), 7.22 (td, *J*₁ = 8.4 Hz, *J*₂ = 2.4 Hz, 1H), 5.29 (q, *J* = 6 Hz, 1H), 1.86 (d, *J* = 6 Hz, 3H); ¹³C NMR (150 MHz, CDCl₃): δ 168.97, 163.12 (d, *J*_{C-F} = 259.5 Hz), 140.16 (d, *J*_{C-F} = 9 Hz), 137.53 (d, *J*_{C-F} = 17 Hz), 134.25 (d, *J*_{C-F} = 9 Hz), 129.71, 129.15, 128.89, 124.10, 115.72 (d, *J*_{C-F} = 22.5 Hz), 115.41 (d, *J*_{C-F} = 22.5 Hz), 73.09, 16.83. HRMS (ESI, *m/z*) calcd. for C₁₅H₁₁O₂F [M + H]⁺: 243.0821; found: 243.0824.

3,9,11-trimethyldibenzo[*c,e*]oxepin-5(7*H*)-one (2m, Scheme 2)

The same general procedures A and B both were followed. Column chromatography (SiO₂, eluting with 97:3 hexane/ethyl acetate) afforded the desired product as a white solid, (39.2 mg, 78% acc. to condition A and 29.2 mg, 58% acc. to condition B). mp 163–165°C. ¹H NMR (400 MHz, CDCl₃): δ 7.69–7.70 (m, 1H), 7.32–7.38 (m, 2H), 7.18 (s, 1H), 7.08 (s, 1H), 4.85 (ABq, *J* = 12 Hz, 2H), 2.43 (s, 3H), 2.37 (s, 3H), 2.36 (s, 3H); ¹³C NMR (100 MHz, CDCl₃): δ 170.98, 137.97, 137.83, 136.47, 135.97, 134.87, 133.58, 133.23, 131.77, 131.48, 131.17, 130.32, 127.01, 70.22, 21.25, 21.06, 21.01. HRMS (ESI, *m/z*) calcd. for C₁₇H₁₅O₂Na [M + Na]⁺: 275.1048; found: 275.1049.

10-Chloro-3-(5-chloro-2-methylphenyl)dibenzo[*c,e*]oxepin-5(7*H*)-one (2n, Scheme 2)

The same general procedures A and B both were followed. Column chromatography (SiO₂, eluting with 97:3 hexane/ethyl acetate) afforded the desired product as a white solid, (55.2 mg, 75% acc. to condition A and 47.0 mg, 64% acc. to condition B). mp > 200°C. ¹H NMR (600 MHz, CDCl₃): δ 7.96 (d, *J* = 1.2 Hz, 1H), 7.70 (s, 1H), 7.61–7.67 (m, 1H), 7.44 (s, 2H), 7.28–7.29 (m, 2H), 7.25–7.23 (m, 1H), 5.05 (ABq, *J* = 12.6 Hz, 2H), 2.29 (s, 3H); ¹³C NMR (150 MHz, CDCl₃): δ 169.47, 141.59, 141.06, 140.24, 136.10, 134.83, 133.73, 133.31, 133.19, 132.59, 131.89, 131.58, 130.67, 130.01, 129.43, 128.73, 128.63, 128.56, 128.01, 68.42, 19.88. HRMS (ESI, *m/z*) calcd. for C₂₁H₁₅O₂Cl₂ [M + H]⁺: 369.0449; found: 369.0453.

7-methyldibenzo[*c,e*]oxepin-5(7*H*)-one (2o, Scheme 2)

The same general procedures **A** and **B** both were followed. Column chromatography (SiO₂, eluting with 97:3 hexane/ethyl acetate) afforded the desired product as a white solid, (22.8 mg, 51% acc. to condition **A** and 24.6 mg, 55% acc. to condition **B**). mp 148–150°C. ¹H NMR (400 MHz, CDCl₃): δ 7.97 (d, *J* = 8 Hz, 1H), 7.65 (td, *J*₁ = 8 Hz, *J*₂ = 1.2 Hz, 1H), 7.59 (td, *J*₁ = 8 Hz, *J*₂ = 1.2 Hz, 2H), 7.44–7.55 (m, 4H), 5.27 (q, *J* = 6.4 Hz, 1H), 1.84 (d, *J* = 6.4 Hz, 3H); ¹³C NMR (100 MHz, CDCl₃): δ 170.04, 138.77, 137.64, 137.44, 132.58, 131.42, 131.01, 129.66, 129.05, 128.87, 128.64, 128.46, 124.03, 73.19, 16.96. HRMS (ESI, *m/z*) calcd. for C₁₅H₁₃O₂ [M + H]⁺: 225.0916; found: 225.0919.

10-chlorodibenzo[*c,e*]oxepin-5(7*H*)-one (2p, Scheme 2)

The same general procedures **A** and **B** both were followed. Column chromatography (SiO₂, eluting with 97:3 hexane/ethyl acetate) afforded the desired product as a white solid, (34.6 mg, 71% acc. to condition **A** and 33.2 mg, 68% acc. to condition **B**). mp 154–156°C. ¹H NMR (600 MHz, CDCl₃): δ 8.00 (d, *J* = 12 Hz, 1H), 7.69 (t, *J* = 7.8 Hz, 1H), 7.64 (s, 1H), 7.55–7.60 (m, 2H), 7.41 (s, 2H), 4.99 (d(br), *J* = 24 Hz, 2H); ¹³C NMR (150 MHz, CDCl₃): δ 169.75, 140.61, 136.00, 135.90, 133.22, 132.74, 132.14, 130.67, 129.92, 129.06, 128.60, 128.57, 68.33. HRMS (ESI, *m/z*) calcd. for C₁₄H₁₀O₂Cl [M + Na]⁺: 245.0369; found: 245.0372.

9,11-dimethyldibenzo[*c,e*]oxepin-5(7*H*)-one (2q, Scheme 2)

The same general procedures **A** with additional amount of 2.0 equiv TEMPO and **B** both were followed. Column chromatography (SiO₂, eluting with 97:3 hexane/ethyl acetate) afforded the desired product as a white solid, (38.4 mg, 81% acc. to condition **A** and 33.2 mg, 70% acc. to condition **B**). ¹H NMR (600 MHz, CDCl₃): δ 7.90 (d, *J* = 7.8 Hz, 1H), 7.58 (t, *J* = 6H, 1H), 7.47 (t, *J* = 7.8 Hz, 2H), 7.21 (s, 1H), 7.11 (s, 1H), 4.89 (AB_q, *J* = 12 Hz, 2H), 2.39 (s, 3H), 2.38 (s, 3H); ¹³C NMR (150 MHz, CDCl₃): δ 170.68, 138.04, 136.43, 136.41, 135.92, 135.90, 134.69, 133.53, 131.53, 130.75, 130.25, 127.78, 126.95, 70.09, 21.13, 20.93. HRMS (ESI, *m/z*) calcd. for C₁₆H₁₅O₂ [M + H]⁺: 239.1072; found: 239.1079.

3-Methoxy-[1,3]dioxolo[4',5':4,5]benzo[1,2-*c*]benzo[*e*]oxepin-5(7*H*)-one (2r, Scheme 2)

The same general procedures **A** and **B** both were followed. Column chromatography (SiO₂, eluting with 93:7 hexane/ethyl acetate) afforded the desired product as a white solid, (35.2 mg, 62% acc. to condition **A** and 40.8 mg, 72% acc. to condition **B**). mp 178–180°C. ¹H NMR (400 MHz, CDCl₃): δ 7.41–7.43 (m, 2H), 7.17 (dd, *J*₁ = 4.8 Hz, *J*₂ = 2.8 Hz, 1H), 7.03 (s, 1H), 6.03 (s, 2H), 4.87 (AB_q, *J* = 12 Hz, 2H), 3.88 (s, 3H); ¹³C NMR (100 MHz, CDCl₃): δ 170.22, 159.24, 149.25, 147.44, 133.33, 131.44, 130.13, 129.92, 128.45, 120.13, 115.16, 108.79, 108.51, 101.75, 69.11, 55.74. HRMS (ESI, *m/z*) calcd. for C₁₆H₁₂O₅Na [M + Na]⁺: 307.0582; found: 307.0597.

4-fluorodibenzo[*c,e*]oxepin-5(7*H*)-one (2s, Scheme 2)

The same general procedures **A** with additional amount of 2.0 equiv TEMPO and **B** both were followed. Column chromatography (SiO₂, eluting with 19:1 hexane/ethyl acetate) afforded the desired product as a white solid, (30.6 mg, 67% acc. to condition **A** and 23.2 mg, 51% acc. to condition **B**). mp 96–98°C. ¹H NMR (600 MHz, CDCl₃): δ 7.68 (d, *J* = 12 Hz, 1H), 7.63–7.59 (m, 1H), 7.54–7.57 (m, 1H), 7.46–7.48 (m, 2H), 7.39 (d, *J* = 7.2 Hz, 2H), 7.24–7.27 (m, 1H), 5.04 (AB_q, *J* = 12 Hz, 2H); ¹³C NMR (150 MHz, CDCl₃): δ 169.18, 163.23 (d, *J*_{C-F} = 364.5 Hz), 139.01, 137.93, 137.42, 134.88, 132.92 (d, *J*_{C-F} = 9 Hz), 131.58, 130.28, 129.19, 128.82, 128.54, 124.16 (d, *J*_{C-F} = 3Hz), 116.11 (d, *J*_{C-F} = 22 Hz), 68.92. HRMS (ESI, *m/z*) calcd. for C₁₄H₁₀O₂F [M + H]⁺: 229.0665; found: 229.0674.

7-phenyldibenzo[*c,e*]oxepin-5(7*H*)-one (2t, Scheme 2)

The same general procedures **A** and **B** both were followed. Column chromatography (SiO₂, eluting with 97:3 hexane/ethyl acetate) afforded the desired product as a white solid, (47.0 mg, 82% acc. to condition **A** and 40.2 mg, 70% acc. to condition **B**). mp 162–170°C. ¹H NMR (600 MHz, CDCl₃): δ 8.03 (d, *J* = 7.8 Hz, 1H), 7.65–7.75 (m, 3H), 7.58 (t, *J* = 7.2 Hz, 1H), 7.41–7.52 (m, 6H), 7.29 (t, *J* = 7.2 Hz, 1H), 6.79 (d, *J* = 7.8 Hz, 1H), 6.25 (s, 1H); ¹³C NMR (150 MHz, CDCl₃): δ 169.42, 138.56, 138.46, 137.29, 135.73, 132.68, 131.46, 130.73, 129.54, 128.90, 128.78, 128.55, 128.52, 128.45, 128.40, 127.38, 126.97, 78.99. HRMS (ESI, *m/z*) calcd. for C₂₀H₁₄O₂Na [M + Na]⁺: 309.0891; found: 309.0444.

[1,3]dioxolo[4',5':4,5]benzo[1,2-*c*]benzo[*e*]oxepin-5(7*H*)-one (2u, Scheme 2)

The same general procedures **A** and **B** both were followed. Column chromatography (SiO₂, eluting with 93:7 hexane/ethyl acetate) afforded the desired product as a white solid, (36.2 mg, 71% acc. to condition

A and 31.6 mg, 62% acc. to condition B). mp 148–150°C. ¹H NMR (600 MHz, CDCl₃): δ 7.94 (dd, *J*₁ = 8 Hz, *J*₂ = 1.2 Hz, 1H), 7.62 (td, *J*₁ = 7.6 Hz, *J*₂ = 1.6 Hz, 1H), 7.44–7.51 (m, 2H), 7.07 (s, 1H), 6.90 (s, 1H), 6.04 (s, 1H), 4.88 (AB_q, *J* = 12 Hz, 2H); ¹³C NMR (100 MHz, CDCl₃): δ 170.40, 149.31, 147.96, 137.33, 133.45, 132.59, 131.95, 130.53, 129.13, 128.43, 128.12, 108.90, 108.82, 101.86, 68.94. HRMS (ESI, *m/z*) calcd. for C₁₅H₁₁O₄ [M + H]⁺: 255.0657; found: 255.0659.

9,10-bis(benzyloxy)dibenzo[*c,e*]oxepin-5(7H)-one (2v, Scheme 2)

The same general procedures A and B both were followed. Column chromatography (SiO₂, eluting with 19:1 hexane/ethyl acetate) afforded the desired product as a white solid, (71.6 mg, 85% acc. to condition A and 74.2 mg, 88% acc. to condition B). mp 152–154°C. ¹H NMR (400 MHz, CDCl₃): δ 7.94 (dd, *J*₁ = 8 Hz, *J*₂ = 1.6 Hz, 1H), 7.59 (td, *J*₁ = 7.6 Hz, *J*₂ = 1.6 Hz, 1H), 7.31–7.46 (m, 12H), 7.18 (s, 1H), 7.00 (s, 1H), 5.22 (s, 4H), 4.85 (d(br), *J* = 52 Hz, 2H); ¹³C NMR (100 MHz, CDCl₃): δ 170.48, 150.13, 149.33, 137.32, 136.83, 136.76, 132.54, 132.40, 132.09, 130.61, 130.26, 128.72, 128.70, 128.54, 128.46, 128.27, 128.15, 127.98, 127.46, 127.32, 115.39, 114.89, 71.72, 71.52, 68.96. HRMS (ESI, *m/z*) calcd. for C₂₈H₂₃O₄ [M + H]⁺: 423.1596; found: 423.1602.

9-Methoxy-10-methyldibenzo[*c,e*]oxepin-5(7H)-one (2w, Scheme 2)

The same general procedures A with additional amount of 2.0 equiv TEMPO and B both were followed. Column chromatography (SiO₂, eluting with 19:1 hexane/ethyl acetate) afforded the desired product as a white solid, (38.0 mg, 75% acc. to condition A and 38.6 mg, 76% acc. to condition B). mp 160–164°C. ¹H NMR (400 MHz, CDCl₃): δ 7.94 (d, *J* = 8 Hz, 1H), 7.61 (t, *J* = 8 Hz, 1H), 7.40–7.46 (m, 2H), 6.87 (s, 1H), 4.96 (d(br), *J* = 48 Hz, 2H), 3.89 (s, 3H), 2.29 (s, 3H); ¹³C NMR (100 MHz, CDCl₃): δ 170.60, 158.10, 137.55, 133.68, 132.50, 132.08, 130.98, 130.91, 130.39, 128.83, 128.37, 127.66, 109.88, 69.39, 55.69, 16.33. HRMS (ESI, *m/z*) calcd. for C₁₆H₁₄O₃ [M]⁺: 254.0943; found: 254.0916.

9-ethoxydibenzo[*c,e*]oxepin-5(7H)-one (2x, Scheme 2)

The same general procedures A and B both were followed. Column chromatography (SiO₂, eluting with 93:7 hexane/ethyl acetate) afforded the desired product as a white solid, (36.0 mg, 71% acc. to condition A and 37.0 mg, 73% acc. to condition B). mp 100–102°C. ¹H NMR (600 MHz, CDCl₃): δ 7.97 (d, *J* = 7.8 Hz, 1H), 7.63 (td, *J*₁ = 7.8 Hz, *J*₂ = 1.2 Hz, 1H), 7.61 (d, *J* = 7.8 Hz, 1H), 7.49–7.57 (m, 2H), 7.45–7.48 (m, 1H), 6.97–7.06 (m, 2H), 4.97 (d(br), *J* = 73 Hz, 2H), 4.11 (q, *J* = 7.2 Hz, 2H), 1.46 (t, *J* = 7.2 Hz, 3H); ¹³C NMR (150 MHz, CDCl₃): δ 170.39, 159.22, 137.29, 136.07, 132.48, 132.00, 131.19, 130.10, 129.86, 128.29, 127.67, 116.08, 114.31, 69.28, 63.77, 14.73. HRMS (ESI, *m/z*) calcd. for C₁₆H₁₅O₃ [M + H]⁺: 255.1021; found: 255.1021.

3-phenylbenzo[*c*]naphtho[2,1-*e*]oxepin-1(3H)-one (2years, Scheme 2)

The same general procedures A and B both were followed. Column chromatography (SiO₂, eluting with 97:3 hexane/ethyl acetate) afforded the desired product as a white solid, (49.0 mg, 73% acc. to condition A and 51.6 mg, 77% acc. to condition B). mp 184–186°C. ¹H NMR (400 MHz, CDCl₃): δ 8.38 (d, *J* = 8 Hz, 1H), 8.11–8.27 (m, 1H), 7.41–7.79 (m, 9H), 7.31 (td, *J*₁ = 8 Hz, *J*₂ = 1.2 Hz, 1H), 6.81 (d, *J* = 8 Hz, 1H), 6.25 (s, 1H); ¹³C NMR (100 MHz, CDCl₃): δ 167.81, 139.21, 138.76, 135.66, 135.28, 133.19, 132.34, 130.99, 129.23, 128.68, 128.64, 128.38, 128.27, 127.65, 127.26, 126.96, 126.79, 126.09, 124.43, 123.57, 118.92, 117.36, 78.88. HRMS (ESI, *m/z*) calcd. for C₂₄H₁₆O₂Na [M + Na]⁺: 359.1048; found: 359.1057.

6-chlorobenzo[*c*]naphtho[2,1-*e*]oxepin-1(3H)-one (2z, Scheme 2)

The same general procedures A and B both were followed. Column chromatography (SiO₂, eluting with 97:3 hexane/ethyl acetate) afforded the desired product as a white solid, (41.6 mg, 71% acc. to condition A and 42.2 mg, 72% acc. to condition B). mp 188–190°C. ¹H NMR (400 MHz, CDCl₃): δ 8.33 (d, *J* = 8 Hz, 1H), 8.07 (d, *J* = 8 Hz, 1H), 7.91 (d, *J* = 8 Hz, 1H), 7.76 (d, *J* = 1.2 Hz, 1H), 7.67–7.58 (m, 3H), 7.45–7.40 (m, 2H), 4.98 (AB_q, *J* = 12 Hz, 2H); ¹³C NMR (100 MHz, CDCl₃): δ 168.14, 140.95, 136.13, 133.98, 133.93, 133.38, 132.44, 131.18, 129.93, 129.06, 128.80, 128.47, 128.31, 127.92, 127.51, 126.88, 125.42, 68.15. HRMS (ESI, *m/z*) calcd. for C₁₈H₁₂O₂Cl [M + H]⁺: 295.0526; found: 295.0531.

6-Chloro-3-methylbenzo[*c*]naphtho[2,1-*e*]oxepin-1(3H)-one (2aa, Scheme 2)

The same general procedures A with additional amount of 2.0 equiv TEMPO and B both were followed. Column chromatography (SiO₂, eluting with 97:3 hexane/ethyl acetate) afforded the desired product as a white solid, (40.2 mg, 65% acc. to condition A and 33.2 mg, 54% acc. to condition B). mp 160–162°C. ¹H NMR (600 MHz, CDCl₃): δ 8.42 (d, *J* = 8.4 Hz, 1H), 8.08 (d, *J* = 9 Hz, 1H), 7.93 (d, *J* = 8.4 Hz, 1H), 7.76

(d, $J = 8.4$ Hz, 1H), 7.68–7.64 (m, 2H), 7.56–7.61 (m, 3H), 7.51 (t, $J = 7.8$ Hz, 1H), 5.32 (q, $J = 6$ Hz, 1H), 1.88 (d, $J = 6.6$ Hz, 3H); ^{13}C NMR (150 MHz, CDCl_3): δ 168.22, 138.85, 138.05, 135.14, 132.96, 131.99, 130.77, 129.51, 129.29, 128.57, 128.12, 127.69, 127.00, 126.64, 125.93, 123.85, 72.76, 16.53. HRMS (ESI, m/z) calcd. for $\text{C}_{19}\text{H}_{14}\text{O}_2\text{Na}$ [$\text{M} + \text{Na}$] $^+$: 297.0891; found: 297.0898.

o-tolyl 2-hydroxybenzoate (4a, Scheme 3) (Wang et al., 2017)

General procedure six was followed. Column chromatography (SiO_2 , eluting with 96:4 hexane/ethyl acetate) afforded the desired product as a colourless oil, (28.6 mg, 62%). ^1H NMR (400 MHz, CDCl_3): δ 10.56 (s, 1H), 8.12 (dd, $J = 8.0$ Hz, 2.0 Hz, 1H), 7.56 (td, $J = 8.0$ Hz, 1.6 Hz, 1H), 7.27–7.32 (m, 2H), 7.23 (td, $J = 8.0$ Hz, 1.6 Hz, 1H), 7.14 (dd, $J = 8.0$ Hz, 1.2 Hz, 1H), 7.06 (dd, $J = 8.8$ Hz, 1.2 Hz, 1H), 6.99 (td, $J = 7.6$ Hz, 1.2 Hz, 1H), 2.26 (s, 3H); ^{13}C NMR (150 MHz, CDCl_3): δ 168.8, 162.3, 148.8, 136.6, 131.5, 130.43, 130.40, 127.2, 126.7, 121.9, 119.6, 117.9, 111.8, 16.3.

Phenyl 2-hydroxybenzoate (4b, Scheme 3) (Wang et al., 2017)

General procedure six was followed. Column chromatography (SiO_2 , eluting with 96:4 hexane/ethyl acetate) afforded the desired product as a colourless oil, (30.2 mg, 64%). ^1H NMR (600 MHz, CDCl_3): δ 10.53 (s, 1H), 8.10 (d, $J = 7.8$ Hz, 1H), 7.55 (t, $J = 8.4$ Hz, 1H), 7.47 (t, $J = 8.4$ Hz, 2H), 7.33 (t, $J = 7.2$ Hz, 1H), 7.23 (d, $J = 8.4$ Hz, 2H), 7.06 (d, $J = 8.4$ Hz, 1H), 6.99 (t, $J = 7.2$ Hz, 1H); ^{13}C NMR (150 MHz, CDCl_3): δ 168.9, 162.2, 150.1, 136.5, 130.3, 129.6, 126.4, 121.6, 119.4, 117.8, 111.8.

4-(Benzyloxy)phenyl 2-hydroxybenzoate (4c, Scheme 3) (Hossian and Jana, 2016)

General procedure six was followed. Column chromatography (SiO_2 , eluting with 95:5 hexane/ethyl acetate) afforded the desired product as a white solid, (40.8 mg, 64%). ^1H NMR (400 MHz, CDCl_3): δ 10.52 (s, 1H), 8.05 (dd, $J = 8.0$ Hz, 1.6 Hz, 1H), 7.52 (td, $J = 7.8$ Hz, 2.0 Hz, 1H), 7.31–7.44 (m, 5H), 7.10–7.14 (m, 2H), 7.01–7.03 (m, 3H), 6.96 (t, $J = 8.0$ Hz, 1H), 5.07 (s, 2H); ^{13}C NMR (100 MHz, CDCl_3): δ 169.3, 162.2, 156.9, 143.7, 136.8, 136.5, 130.4, 128.7, 128.2, 127.5, 122.5, 119.5, 117.9, 115.7, 111.9, 70.5.

4-Chlorophenyl 2-hydroxybenzoate (4days, Scheme 3) (Hossian and Jana, 2016)

General procedure six was followed. Column chromatography (SiO_2 , eluting with 96:4 hexane/ethyl acetate) afforded the desired product as a white solid, (28.4 mg, 57%). ^1H NMR (600 MHz, CDCl_3): δ 10.40 (s, 1H), 8.05 (d, $J = 7.8$ Hz, 1H), 7.55 (t, $J = 7.8$ Hz, 1H), 7.42 (d, $J = 9.0$ Hz, 2H), 7.17 (d, $J = 9.0$ Hz, 2H), 7.05 (d, $J = 8.4$ Hz, 1H), 6.98 (t, $J = 7.8$ Hz, 1H); ^{13}C NMR (150 MHz, CDCl_3): δ 168.6, 162.2, 148.5, 136.7, 131.8, 130.3, 129.7, 123.0, 119.6, 117.9, 111.5.

4-Methoxyphenyl 2-hydroxybenzoate (4e, Scheme 3) (Wang et al., 2017)

General procedure six was followed. Column chromatography (SiO_2 , eluting with 95:5 hexane/ethyl acetate) afforded the desired product as a colourless oil, (29.4 mg, 61%).

^1H NMR (400 MHz, CDCl_3): δ 10.51 (s, 1H), 8.05 (dd, $J = 8.0$ Hz, 2.0 Hz, 1H), 7.50–7.54 (m, 1H), 7.09–7.12 (m, 2H), 7.02 (dd, $J = 8.0$ Hz, 0.8 Hz, 1H), 6.93–6.97 (m, 3H), 3.82 (s, 3H); ^{13}C NMR (100 MHz, CDCl_3): δ 169.4, 162.2, 157.8, 143.6, 136.5, 130.4, 122.5, 119.5, 117.9, 114.7, 111.9, 55.7.

4-Bromophenyl 2-hydroxybenzoate (4f, Scheme 3) (Hossian and Jana, 2016)

General procedure six was followed. Column chromatography (SiO_2 , eluting with 96:4 hexane/ethyl acetate) afforded the desired product as a white solid, (28.2 mg, 48%). ^1H NMR (400 MHz, CDCl_3): δ 10.36 (s, 1H), 8.03 (dd, $J = 8.0$ Hz, 1.6 Hz, 1H), 7.51–7.57 (m, 3H), 7.08–7.12 (m, 2H), 7.03 (d, $J = 8.4$ Hz, 1H), 6.99 (t, $J = 8.0$ Hz, 1H); ^{13}C NMR (100 MHz, CDCl_3): δ 168.6, 162.3, 149.3, 136.8, 132.7, 130.4, 123.5, 119.6, 119.6, 118.0, 111.6.

Naphthalen-2-yl 2-hydroxybenzoate (4g, Scheme 3) (Hossian and Jana, 2016)

General procedure six was followed. Column chromatography (SiO_2 , eluting with 96:4 hexane/ethyl acetate) afforded the desired product as a white solid, (34.0 mg, 65%). ^1H NMR (400 MHz, CDCl_3): δ 10.51 (s, 1H), 8.13 (dd, $J = 8.0$ Hz, 1.6 Hz, 1H), 7.92 (d, $J = 8.8$ Hz, 1H), 7.83–7.89 (m, 2H), 7.68 (d, $J = 2.4$ Hz, 1H), 7.49–7.58 (m, 3H), 7.34 (dd, $J = 8.8$ Hz, 2.4 Hz, 1H), 7.05 (dd, $J = 8.4$ Hz, 0.8 Hz, 1H), 6.99 (t, $J = 8.4$ Hz, 1H); ^{13}C NMR (100 MHz, CDCl_3): δ 169.2, 162.3, 147.8, 136.6, 133.8, 131.8, 130.5, 129.8, 127.9, 127.8, 126.9, 126.1, 120.9, 119.6, 118.8, 117.9, 111.9.

2-Methoxyphenyl 2-hydroxybenzoate (4h, Scheme 3) (Wang et al., 2017)

General procedure six was followed. Column chromatography (SiO₂, eluting with 95:5 hexane/ethyl acetate) afforded the desired product as a white solid, (26.0 mg, 53%). ¹H NMR (400 MHz, CDCl₃): δ 10.47 (s, 1H), 8.10 (dd, *J* = 8.0 Hz, 1.2 Hz, 1H), 7.50–7.54 (m, 1H), 7.25–7.29 (m, 1H), 7.15 (dd, *J* = 8.0 Hz, 1.6 Hz, 1H), 7.00–7.04 (m, 3H), 6.99–6.94 (m, 1H), 3.82 (s, 3H); ¹³C NMR (100 MHz, CDCl₃): δ 168.5, 162.1, 151.2, 139.2, 136.3, 130.7, 127.5, 122.9, 120.9, 119.5, 117.8, 112.7, 111.9, 56.0.

3-Methoxyphenyl 2-hydroxybenzoate (4i, Scheme 3) (Hossian and Jana, 2016)

General procedure six was followed. Column chromatography (SiO₂, eluting with 95:5 hexane/ethyl acetate) afforded the desired product as a colourless oil, (34.0 mg, 68%). ¹H NMR (400 MHz, CDCl₃): δ 10.48 (s, 1H), 8.06 (dd, *J* = 8.0 Hz, 1.6 Hz, 1H), 7.53 (td, *J* = 8.4 Hz, 1.6 Hz, 1H), 7.34 (t, *J* = 8.0 Hz, 1H), 7.02 (dd, *J* = 8.0 Hz, 0.8 Hz, 1H), 6.96 (td, *J* = 8.0 Hz, 1.2 Hz, 1H), 6.84–6.87 (m, 1H), 6.78–6.81 (m, 1H), 6.76 (t, *J* = 2.4 Hz, 1H), 3.82 (s, 3H); ¹³C NMR (100 MHz, CDCl₃): δ 168.9, 162.3, 160.7, 151.1, 136.5, 130.4, 130.1, 119.5, 117.9, 113.8, 112.3, 111.9, 107.8, 55.58.

Phenyl 4-chloro-2-hydroxybenzoate (4j, Scheme 3) (Hossian and Jana, 2016; Wang et al., 2017)

General procedure six was followed. Column chromatography (SiO₂, eluting with 96:4 hexane/ethyl acetate) afforded the desired product as a colourless oil, (30.0 mg, 61%). ¹H NMR (400 MHz, CDCl₃): δ 10.62 (s, 1H), 8.03 (d, *J* = 8.8 Hz, 1H), 7.46–7.50 (m, 2H), 7.34 (t, *J* = 7.2 Hz, 1H), 7.22–7.24 (m, 2H), 7.09 (d, *J* = 2.0 Hz, 1H), 6.98 (dd, *J* = 8.4 Hz, 2.0 Hz, 1H); ¹³C NMR (100 MHz, CDCl₃): δ 168.4, 162.7, 150.0, 142.4, 131.4, 129.7, 126.6, 121.6, 120.3, 118.1, 110.6.

Phenyl 2-hydroxy-4-nitrobenzoate (4k, Scheme 3) (Hossian and Jana, 2016)

General procedure six was followed. Column chromatography (SiO₂, eluting with 9:1 hexane/ethyl acetate) afforded the desired product as a yellowish solid, (25.8 mg, 50%). ¹H NMR (400 MHz, CDCl₃): δ 10.71 (s, 1H), 8.25 (d, *J* = 8.8 Hz, 1H), 7.86 (d, *J* = 2.0 Hz, 1H), 7.78 (dd, *J* = 8.8 Hz, 2.0 Hz, 1H), 7.47 (t, *J* = 7.6 Hz, 2H), 7.34 (tt, *J* = 7.6 Hz, 1.2 Hz, 1H), 7.20–7.23 (m, 2H); ¹³C NMR (100 MHz, CDCl₃): δ 167.7, 162.6, 153.0, 149.7, 131.8, 129.9, 127.0, 121.4, 116.7, 113.8, 113.4.

Phenyl 2-hydroxy-5-nitrobenzoate (4L, Scheme 3) (Hossian and Jana, 2016)

General procedure six was followed. Column chromatography (SiO₂, eluting with 9:1 hexane/ethyl acetate) afforded the desired product as a yellowish solid, (26 mg, 50%). ¹H NMR (400 MHz, CDCl₃): δ 11.16 (s, 1H), 9.02 (d, *J* = 2.8 Hz, 1H), 8.40 (dd, *J* = 9.2 Hz, 2.8 Hz, 1H), 7.47 (t, *J* = 8.0 Hz, 2H), 7.34 (tt, *J* = 7.2 Hz, 1.2 Hz, 1H), 7.21–7.24 (m, 2H), 7.15 (d, *J* = 9.2 Hz, 1H); ¹³C NMR (100 MHz, CDCl₃): δ 167.8, 166.7, 149.7, 140.3, 131.2, 129.9, 127.1, 127.0, 121.4, 119.0, 111.8.

4-Chlorophenyl 2-hydroxy-5-nitrobenzoate (4m, Scheme 3) (Hossian and Jana, 2016)

General procedure six was followed. Column chromatography (SiO₂, eluting with 9:1 hexane/ethyl acetate) afforded the desired product as a white solid, (28.2 mg, 45%). ¹H NMR (400 MHz, CDCl₃): δ 11.03 (s, 1H), 8.98 (d, *J* = 2.8 Hz, 1H), 8.41 (dd, *J* = 9.2 Hz, 2.8 Hz, 1H), 7.42–7.45 (m, 2H), 7.17–7.19 (m, 2H), 7.15 (d, *J* = 9.2 Hz, 1H); ¹³C NMR (100 MHz, CDCl₃): δ 167.5, 166.7, 148.1, 140.3, 132.6, 131.4, 130.0, 127.1, 122.8, 119.1, 111.5.

7-Methoxy-2,2-dimethyl-4-oxo-4H-benzo[d][1,3]dioxin-5-yl trifluoromethanesulfonate (9)

¹H NMR (400 MHz, CDCl₃): δ 6.47 (d, *J* = 8 Hz, 2H), 3.84 (s, 3H), 1.69 (s, 6H); ¹³C NMR (100 MHz, CDCl₃): δ 165.70, 158.92, 157.20, 149.93, 123.58, 120.38, 117.19, 114.00, 106.67, 105.42, 105.41, 105.40, 101.20, 100.94, 56.39, 25.53; ¹⁹F NMR (376 Hz, CDCl₃): δ –73.06.

2-(4,5-bis(benzyloxy)-2-methylphenyl)-4,4,5,5-tetramethyl-1,3,2-dioxaborolane (13)

¹H NMR (400 MHz, CDCl₃): δ 7.24–7.48 (m, 12H), 5.15 (s, 2H), 5.13 (s, 2H), 2.46 (s, 3H), 1.32 (s, 12H); ¹³C NMR (100 MHz, CDCl₃): δ 151.29, 146.19, 139.91, 137.80, 137.35, 128.52, 127.72, 127.30, 122.90, 116.50, 83.34, 71.92, 70.84, 24.99, 21.82.

5-(4,5-bis(benzyloxy)-2-methylphenyl)-7-methoxy-2,2-dimethyl-4H-benzo[d][1,3]dioxin-4-one (14)

¹H NMR (400 MHz, CDCl₃): δ 7.26–7.48 (m, 10H), 6.83 (s, 1H), 6.72 (s, 1H), 6.43 (d, *J* = 2.4 Hz, 1H), 6.37 (d, *J* = 2.4 Hz, 1H), 5.05–5.20 (m, 4H), 3.81 (s, 3H), 2.03 (s, 3H), 1.72 (s, 6H); ¹³C NMR (100 MHz, CDCl₃): δ 164.67, 158.96, 158.61,

148.64, 146.89, 146.59, 137.65, 133.18, 128.52, 128.50, 128.43, 127.78, 127.70, 127.65, 127.49, 116.43, 113.14, 105.85, 105.11, 100.68, 71.99, 71.40, 55.77, 26.26, 25.32, 19.52. HRMS (ESI, m/z) calcd. for $C_{32}H_{31}O_6$ [M + H]⁺: 511.2121; found: 511.2123.

3,4',5'-tris(benzyloxy)-5-methoxy-2'-methyl-[1,1'-biphenyl]-2-carboxylic acid (16)

¹H NMR (400 MHz, CDCl₃): δ 7.27–7.46 (m, 15H), 6.80 (s, 1H), 6.75 (s, 1H), 6.53 (d, $J = 2.4$ Hz, 1H), 6.31 (d, $J = 2.4$ Hz, 1H), 5.07–5.15 (m, 6H), 3.77 (s, 3H), 2.04 (s, 3H); ¹³C NMR (100 MHz, CDCl₃): δ 163.55, 161.63, 157.73, 148.46, 146.22, 144.77, 137.58, 135.79, 133.30, 128.83, 128.52, 128.43, 127.79, 127.65, 127.58, 127.44, 116.50, 116.35, 108.30, 99.17, 71.58, 71.38, 71.32, 55.64, 19.59.

4,9,10-tris(benzyloxy)-2-methoxydibenzo[c,e]oxepin-5(7H)-one (17)

¹H NMR (400 MHz, CDCl₃): δ 7.29–7.48 (m, 15H), 7.14 (s, 1H), 6.96 (s, 1H), 6.55 (d, $J = 2$ Hz, 1H), 6.32 (d, $J = 2$ Hz, 1H), 5.11–5.28 (m, 6H), 4.80 (AB_q, $J = 12$ Hz, 2H), 3.77 (s, 3H); ¹³C NMR (100 MHz, CDCl₃): δ 166.67, 162.30, 159.46, 149.73, 149.43, 139.80, 137.01, 136.77, 136.43, 132.14, 130.23, 129.20, 128.74, 128.73, 128.69, 128.67, 128.55, 128.14, 128.04, 127.94, 127.40, 127.32, 127.17, 127.14, 127.13, 115.47, 114.74, 114.03, 104.81, 100.50, 71.74, 71.50, 71.18, 68.22, 55.60. HRMS (ESI, m/z) calcd. for $C_{16}H_{31}O_6$ [M + H]⁺: 559.2121; found: 559.2132.

4,9,10-Trihydroxy-2-methoxydibenzo[c,e]oxepin-5(7H)-one, alterlactone (18)

(Cudaj and Podlech, 2012) ¹H NMR (600 MHz, DMSO-*d*₆): δ 10.21 (br s, 1H), 9.47 (br s, 1H), 9.38 (br s, 1H), 7.04 (s, 1H), 6.91 (s, 1H), 6.51 (d, $J = 2.4$ Hz, 1H), 6.46 (d, $J = 2.4$ Hz, 1H), 4.87–4.79 (m, 2H), 3.82 (s, 3H); ¹³C NMR (100 MHz, DMSO-*d*₆): δ 168.77, 162.26, 159.99, 146.60, 145.91, 140.08, 129.88, 126.65, 115.55, 109.48, 105.08, 100.83, 67.84, 55.41. HRMS (EI, m/z) calcd. for $C_{15}H_{12}O_6$ [M + H]⁺: 288.0634; found: 288.0636. Spectroscopic data is in full accordance with the reported one.

Dibenzo[c,e]oxepan-5-thione (DOT, 19) (Bingham and Roth, 2019)

¹H NMR (600 MHz, CDCl₃): δ 8.18 (d, $J = 8.4$ Hz, 1H), 7.66 (d, $J = 7.2$ Hz, 1H), 7.62 (t, $J = 8.4$ Hz, 1H), 7.52–7.57 (m, 2H), 7.46 (t, $J = 6.6$ Hz, 3H), 5.20 (AB_q, $J = 1.2$ Hz, 2H); ¹³C NMR (150 MHz, CDCl₃): δ 216.04, 139.06, 134.55, 134.49, 133.93, 132.05, 130.30, 128.74, 128.55, 128.40, 128.07, 73.79.

2'-(hydroxymethyl)-[1,1'-biphenyl]-2-carboxylic acid (20)

¹H NMR (400 MHz, DMSO-*d*₆): δ 7.84 (dd, $J_1 = 2$ Hz, $J_2 = 1.6$ Hz, 1H), 7.47 (qd, $J_1 = 8$ Hz, $J_2 = 1.6$ Hz, 2H), 7.38 (td, $J_1 = 8$ Hz, $J_2 = 1.6$ Hz, 1H), 7.27 (td, $J_1 = 8$ Hz, $J_2 = 1.6$ Hz, 1H), 7.18 (tt, $J_1 = 7.2$ Hz, $J_2 = 1.6$ Hz, 2H), 6.96 (dd, $J_1 = 7.6$ Hz, $J_2 = 1.2$ Hz, 1H), 4.81 (br s, 1H), 4.30 (AB_q, $J = 13.2$ Hz, 2H); ¹³C NMR (100 MHz, DMSO-*d*₆): δ 169.76, 141.31, 140.33, 138.35, 131.44, 131.01, 130.90, 129.52, 128.56, 127.19, 127.15, 126.83, 126.39, 61.79.

2,6-Dimethyl-3'H-spiro[cyclohexane-1,1'-isobenzofuran]-2,5-diene-3',4-dione (24) (Li et al., 2019)

¹H NMR (400 MHz, CDCl₃): δ 7.97 (dt, $J_1 = 7.6$ Hz, $J_2 = 1.2$ Hz, 1H), 7.69 (td, $J_1 = 8.1$ Hz, $J_2 = 1.2$ Hz, 1H), 7.61 (td, $J_1 = 7.6$ Hz, $J_2 = 1.2$ Hz, 1H), 7.17 (dt, $J_1 = 8.0$ Hz, $J_2 = 1.2$ Hz, 1H), 6.24 (s, 2H), 1.62 (s, 6H); ¹³C NMR (100 MHz, CDCl₃): δ 184.9, 169.9, 154.6, 148.1, 135.4, 130.6, 128.3, 126.3, 126.4, 121.5, 85.0, 17.2.

*6a-methyl-5H-benzo[4,5][1,3]oxazino[3,2-*a*]indole-5,7(6aH)-dione (25)*

¹H NMR (400 MHz, CDCl₃): δ 8.14 (dd, $J_1 = 8.0$ Hz, $J_2 = 1.6$ Hz, 1H), 7.72–7.79 (m, 2H), 7.60 (t, $J = 8.0$ Hz, 1H), 7.53 (d, $J = 8.0$ Hz, 1H), 7.37 (d, $J = 8$ Hz, 1H), 7.30 (td, $J_1 = 8$ Hz, $J_2 = 1.2$ Hz, 1H), 7.08 (t, $J = 8$ Hz, 1H), 1.70 (s, 3H); ¹³C NMR (100 MHz, CDCl₃): δ 192.9, 161.3, 155.3, 139.4, 138.5, 135.7, 131.5, 126.5, 124.8, 122.5, 121.4, 120.1, 117.3, 109.9, 90.9, 19.5.

HRMS (ESI, m/z) calcd. for $C_{16}H_{11}NO_3$ [M + H]⁺: 266.0817; found: 266.0812.

4-Methyl-9H-fluoren-9-one (27) (Fukuyama et al., 2014)

¹H NMR (400 MHz, CDCl₃): δ 7.68–7.69 (m, 1H), 7.62 (d, $J = 8$ Hz, 1H), 7.51–7.53 (m, 1H), 7.45–7.49 (m, 1H), 7.24–7.29 (m, 2H), 7.17 (t, $J = 7.6$ Hz, 3H), 2.58 (s, 3H); ¹³C NMR (100 MHz, CDCl₃): δ 194.3, 145.4, 142.2, 137.4, 134.7, 134.6, 134.5, 133.7, 128.8, 128.4, 124.3, 123.4, 122.0, 20.3.

6-(phenylsulfonyl)-6,7-dihydro-5H-dibenzo[c,e]azepin-5-one (29)

¹H NMR (400 MHz, CDCl₃) δ 7.87 (dd, *J*₁ = 8 Hz, *J*₂ = 1.6 Hz, 1H), 7.65–7.68 (m, 3H), 7.44–7.61 (m, 7H), 7.30 (t, *J* = 8 Hz, 2H), 5.40 (d, *J* = 15.2 Hz, 1H), 4.45 (d, *J* = 15.2 Hz, 1H); ¹³C NMR (100 MHz, CDCl₃): δ 168.52, 136.37, 136.07, 133.58, 132.47, 131.01, 129.58, 129.31, 128.94, 128.79, 128.64, 128.54, 128.50, 128.31, 128.05, 48.06. HRMS (ESI, *m/z*) calcd. for C₂₀H₁₅NO₃S [M + H]⁺: 350.0851; found: 350.0842.

(E)-3-Styrylisobenzofuran-1(3H)-one (31) (Krätzschar et al., 2015)

¹H NMR (400 MHz, CDCl₃): δ 7.94 (d, *J* = 8 Hz, 1H), 7.70 (td, *J*₁ = 7.6 Hz, 1H), 7.45–7.59 (m, 7H), 6.93 (d, *J* = 15.6 Hz, 1H), 6.24 (dd, *J*₁ = 16 Hz, *J*₂ = 7.6 Hz, 1H), 6.01 (d, *J* = 7.2 Hz, 1H); ¹³C NMR (100 MHz, CDCl₃): δ 170.15, 148.42, 138.94, 134.43, 133.40, 130.69, 130.36, 129.73, 127.15, 126.71, 126.04, 125.81, 125.79, 122.64, 81.44.